



JGR Biogeosciences

RESEARCH ARTICLE

10.1029/2020JG005824

Key Points:

- Fens have repeatedly undergone permafrost aggradation and degradation over the last 500 years, but future permafrost formation is unlikely
- Groundwater promoted widespread, long-term permafrost degradation, while climate extremes caused recent permafrost aggradation, but only in late successional stages
- Climate, hydrology, ecosystem, and permafrost interactions complicate ecological transitions and soil carbon changes across the peatlands

Supporting Information:

· Supporting Information S1

Correspondence to:

M. T. Jorgenson, ecoscience@alaska.net

Citation:

Jorgenson, M. T., Douglas, T. A., Liljedahl, A. K., Roth, J. E., Cater, T. C., Davis, W. A., et al. (2020). The roles of climate extremes, ecological succession, and hydrology in repeated permafrost aggradation and degradation in fens on the Tanana Flats, Alaska. *Journal of Geophysical Research: Biogeosciences*, 125, e2020JG005824. https://doi.org/10.1029/2020JG005824

Received 5 MAY 2020 Accepted 29 SEP 2020 Accepted article online 18 NOV 2020

Author Contributions:

Conceptualization: M. Torre Jorgenson, Charles H. Racine Formal analysis: M. Torre Jorgenson Investigation: M. Torre Jorgenson, Thomas A. Douglas, Anna K. Liljedahl, Joanna E. Roth, Tim C. Cater, Wendy A. Davis, Gerald V. Frost, Patricia F. Miller, Charles H. Racine Writing – original draft: M. Torre

Writing – review & editing: Thomas A. Douglas, Anna K. Liljedahl, Gerald V. Frost

©2020. American Geophysical Union. All Rights Reserved.

The Roles of Climate Extremes, Ecological Succession, and Hydrology in Repeated Permafrost Aggradation and Degradation in Fens on the Tanana Flats, Alaska

M. Torre Jorgenson¹, Thomas A. Douglas², Anna K. Liljedahl³, Joanna E. Roth⁴, Tim C. Cater⁴, Wendy A. Davis⁴, Gerald V. Frost⁴, Patricia F. Miller⁴, and Charles H. Racine⁵

¹Alaska Ecoscience, Fairbanks, AK, USA, ²U.S. Army Cold Regions Research and Engineering Laboratory, Fort Wainwright, AK, USA, ³Woods Hole Research Center, Woods Hole, MA, USA, ⁴ABR, Inc-Environmental Research and Services, Fairbanks, AK, USA, ⁵U.S. Army Cold Regions Research and Engineering Laboratory, Hanover, NH, USA

Abstract The Tanana Flats in central Alaska are a hot spot for thermokarst that is rapidly transforming the landscape. Time series analysis of high-resolution imagery showed that permafrost degradation increased the area of three large fens by 26% from 1949 to 2018, but surprisingly permafrost also aggraded in small areas. Permafrost soils in adjacent birch forests frequently had fen peat near the surface indicating recent permafrost degradation and aggradation. We attribute groundwater as the primary driver of recent permafrost degradation, while climate extremes (especially cold, less snowy winters) caused recent permafrost aggradation, but only after ecological succession provided conditions favorable for permafrost formation. Near-surface groundwater temperatures during early winters (2-6°C during 2011-2014) contributed to a near steady rate of lateral permafrost degradation (0.36 m/yr) over three periods. Fairbanks climate records (1904-2019) showed large ranges in mean winter temperatures (12°C) and snow depths (69 cm) between cold, less snowy winters and warm, snowy winters. During ecological succession from the collapsing margins to the fen centers over a ~250-yr period, vegetation transitioned from aquatic forbs to shrubs and mosses, water depths decreased, and the soil carbon stock of new peat increased. These interactions among permafrost, groundwater, climate warming, and succession complicate our ability to project future ecological transitions and soil carbon changes across this dynamic boreal lowland landscape. The more frequent warm, snowy winters since 2014 and model projections for warmer winters, however, indicate that the region has crossed a tipping point where permafrost will no longer form and permafrost loss is irreversible.

1. Introduction

The Tanana Flats in central Alaska is a hot spot for thermokarst, ground collapse caused by thawing of ice-rich permafrost, that is rapidly transforming the hydrology and ecology of this boreal lowland landscape (Douglas et al., 2015; Jorgenson et al., 2001; Lara et al., 2015; Racine & Walters, 1994). Similar thermokarst fens are widespread in boreal lowlands in Alaska (Jorgenson et al., 2013; Jorgenson, Shur, et al., 2007), Canada (Payette et al., 2004; Quinton et al., 2011; Thie, 1974), Scandinavia (Lindholm & Heikkilä, 2006) and Russia (Glagolev et al., 2011; Olefeldt et al., 2016) due to the hydrothermal effects of groundwater movement (Sjöberg et al., 2016; Walvoord & Kurylyk, 2016). While climate change (winter and summer air temperature and wintertime snowpack) and groundwater hydrology have been attributed to be the main drivers of rapid permafrost degradation leading to the development of thermokarst fens, bogs, and lakes (Hayashi et al., 2004; Jorgenson et al., 2001; Payette et al., 2004), ecological feedbacks (canopy cover effects on microclimate, and moss and peat accumulation on thermal regimes) also are important in controlling permafrost dynamics in boreal peatland ecosystems (Runyan & D'Odorico, 2012; Zoltai, 1993).

Climate warming is having pronounced effects on soil and water hydrogeologic processes in regions underlain by discontinuous permafrost (Burn & Jorgenson, 2020; Douglas et al., 2020; Jorgenson et al., 2010; Osterkamp et al., 2000). A 4–6°C increase in mean annual air temperatures is projected for interior Alaska by 2,100 (Walsh et al., 2018) and most permafrost is projected to disappear (Pastick et al., 2015). Widespread permafrost degradation has contributed to major changes in vegetation (Jorgenson, Marcot, et al., 2015; Wolken et al., 2011), biological and physical processes in soils (Harden et al., 2012; McGuire

JORGENSON ET AL. 1 of 23



et al., 2018), and hydrogeologic processes (Kane et al., 2010; O'Donnell et al., 2012; Petrone et al., 2006; Walvoord & Kurylyk, 2016).

Surface water features, such as rivers, lakes, streams, bogs, fens, and other wetlands exhibit heterogeneous responses to climate warming or disturbance, such as wildfire or human development, across the landscape (Jorgenson et al., 2013; Jorgenson, Marcot, et al., 2015; Roach et al., 2011). Water features underlain or surrounded by permafrost exhibit an intense seasonality in their flow paths, discharge rates, and biogeochemistry (Barker et al., 2014; Douglas et al., 2013; Petrone et al., 2006; Walvoord & Striegl, 2007). Of particular note on a global scale is the large amount of soil carbon currently stored in circumpolar peatlands that could be mobilized if permafrost thaws or terrestrial exports to rivers are altered by hydrologic regime changes (Hugelius et al., 2014; Vonk et al., 2019; Walvoord & Striegl, 2007). Permafrost peatland fen systems are hot spots for export of dissolved organic carbon out of permafrost landscapes so the seasonality of fen hydrology has major ramifications on downstream nutrient processes (Olefeldt & Roulet, 2014).

Groundwater hydrology is greatly affected by permafrost, which controls surface, shallow subsurface, and deep flow paths (Walvoord & Kurylyk, 2016). Due to the extremely flat topography of permafrost lowlands like the Tanana Flats (<1 m of elevation change per kilometer), there could be marked changes in the future hydrogeologic regime where permafrost degrades or thermokarst (ground subsidence following degradation of ice-rich permafrost) occurs. Because permafrost and seasonally frozen soils have extremely low hydraulic conductivities, the soil storage of surface water and subsurface flow rates also are affected by changes in the timing and rate of seasonal subsurface thawing (Quinton et al., 2008; Woo, 2012). For example, Alaska subsidence-driven landscape elevation changes of as small as 0.5 m drastically increased runoff and reduced storage at low gradient sites in northern Alaska (Liljedahl et al., 2016). The hydrogeologic response to permafrost extent and degradation is most likely quantifiable in late summer when the seasonal thawing is greatest (Wright et al., 2009). Permafrost can affect deeper flow paths and riverine geochemistry because permafrost bodies channel subsurface flows and control sources of weathered soils and bedrock (Douglas et al., 2013; Vonk et al., 2019). Thus, where permafrost degrades the patterns of water storage and surface and subsurface flows are dramatically reorganized (Jorgenson et al., 2013; Liljedahl et al., 2016).

Fens associated with degrading permafrost, variously termed thermokarst fens (Jorgenson, 2013) or collapse-scar fens (NWWG, 1988), are broad linear features tens to hundreds of meters wide and kilometers long with a floating peat mat (Jorgenson et al., 1999; Quinton et al., 2009). They are often hydrologically linked to lakes and ponds and they play major roles in nutrient cycling between aquatic and terrestrial ecosystems (Fan et al., 2013; Rober et al., 2014). Fen soil typically are composed of a sequence of high hydraulic conductivity peats, low-conductivity fine-grained sediments and higher conductivity sands or gravels that promote major lateral (surface) flow conduits (Hayashi et al., 2004; Jorgenson et al., 2001; Quinton et al., 2009). In permafrost terrain, channel fens are laterally constrained by ice-rich peat plateaus that are elevated 1 to 2 m above the fens (Quinton et al., 2003; Racine & Walters, 1994). Permafrost degradation reduces the effects of the permafrost aquiclude which could alter regional and local hydraulic gradients (Jepsen et al., 2013; Yoshikawa & Hinzman, 2003). In mountainous regions, fens can be strongly coupled to regional hydrologic pathways, such as the Tanana Flats downslope of the Alaska Range (Ferrick et al., 2008; Racine & Walters, 1994). Surface water can play a role as a source of heat to thaw permafrost but also, as seasonal thaw progresses and over time as permafrost thaws, surface water can move into the shallow subsurface.

Fen ecosystems are geogenous peatlands influenced by surface or ground water flows that have been in contact with mineral soils (Lindholm & Heikkilä, 2006; NWWG, 1988). Fen ecosystems have minerotrophic vegetation dominated by herbaceous species, particularly forbs, sedges, and horsetails, with vegetation patterns mainly controlled by water levels, nutrient availability, and distance from the wetland margin (Bubier, 1995; Racine, Jorgenson, et al., 1998). Biogeochemical processes are highly sensitive to water table fluctuations, particularly when the fens are capped by a floating mat (Bubier, 1995; Roulet et al., 1992; Sulman et al., 2010; Turetsky et al., 2008). Nutrients and base content strongly drive species composition and form the basis for differentiating rich and poor fens (Lindholm & Heikkilä, 2006; NWWG, 1988). In interior Alaska, fens also provide important habitat for moose and waterbirds, and serve as waterways for human access to what is otherwise inaccessible terrain (Boertje et al., 2000; Jorgenson, Murphy, et al., 2007; Racine, Walters, et al., 1998).

JORGENSON ET AL. 2 of 23

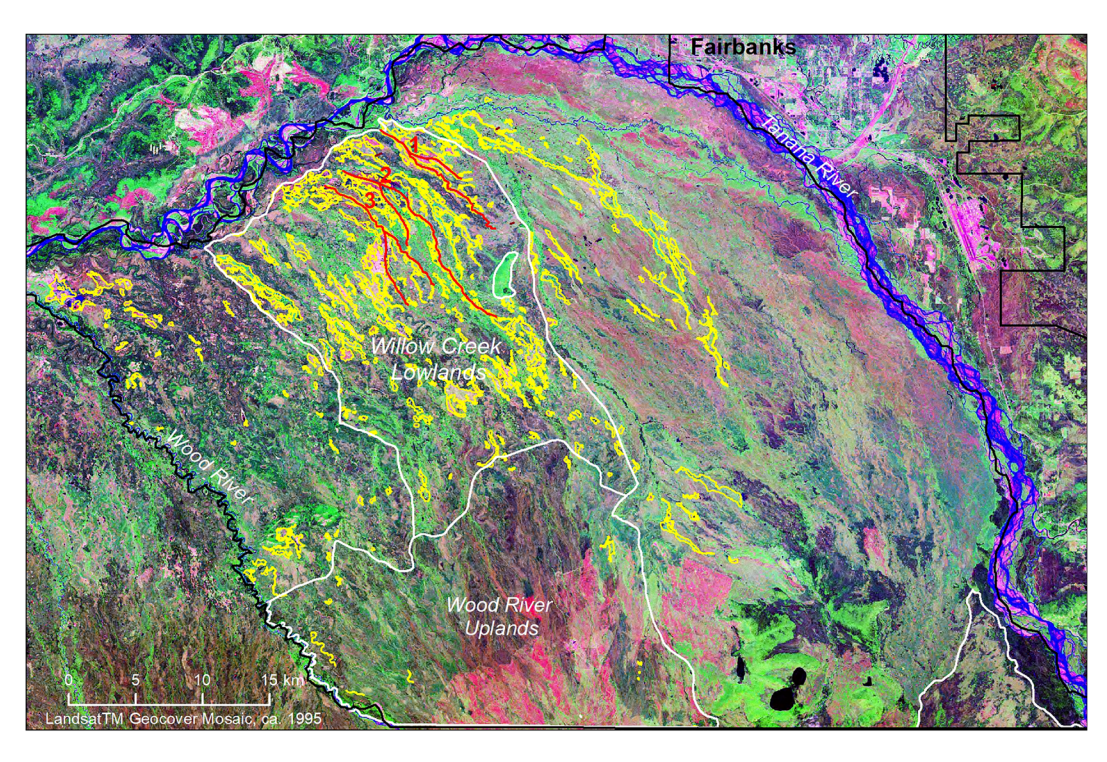


Figure 1. Map of overall fen distribution (yellow, from Jorgenson et al. 1998) and the three sampled fen systems (centerlines in red) on the Tanana Flats, Central Alaska. Ft. wainwright boundaries are in black and ecological landscapes in white, with only landscapes of primary interest delineated and labeled.

Here, we use remote sensing of permafrost degradation, soil and vegetation sampling, surface and ground-water monitoring, and long-term climate records to evaluate the relative roles of climate, ecological succession, and hydrology in controlling permafrost aggradation and degradation in thermokarst channel fens. The Specific objectives of this study were to (1) determine short-term (1949–2018) trends in permafrost aggradation and degradation through analysis of high-resolution satellite and aerial imagery; (2) evaluate soil and permafrost stratigraphy to identify previous thermokarst episodes over the late Holocene; (3) identify patterns of ecological succession within the fens; (4) quantify seasonal hydrologic and thermal regimes; (5) analyze climate data to identify specific winter and summer seasons of extreme temperature and precipitation that affected permafrost dynamics; and (6) evaluate patterns of permafrost aggradation and degradation in relation to climate, ecological succession, and near-surface hydrothermal regimes.

2. Study Area

The study focused on fens on the Tanana Flats lowlands (\sim 8,000 km 2), which extend northward \sim 100 km from the northern slopes of the Alaska Range to the Tanana River. Most of the area is contained within the Tanana Flats Training Area of Ft Wainwright (Figure 1), where work was conducted in support of the Army's natural resource management objectives.

The climate at Fairbanks (\sim 20 km north of study area) is continental, with a mean annual air temperature of -2.4° C (1904–2019), mean monthly temperatures of 16.0°C in July and -21.9° C in January, and extremes ranging from -51° C to 29°C (https://www.ncdc.noaa.gov/cdo-web/). Mean annual precipitation is 303 mm with 40–45% of this as snow (Liston & Hiemstra, 2011).

Geologically, the Tanana Flats is a complex of fluvial deposits associated with a large outwash fan in the western portion of the area and braided floodplain deposits in the northern and eastern portion of the area (Jorgenson et al., 1999; Walters et al., 1998). Much of the area has a typical stratigraphic sequence of peat (0.5–1.5 m), eolian silt (2–3 m), and alluvial sand and gravel (Jorgenson et al., 1999). Permafrost covers about 44% of the area (Jorgenson et al., 2001). Permafrost excess ice contents in birch forests can be greater than 50%, while ice contents in the black spruce stands are typically closer to 20% (Brown et al., 2015;

JORGENSON ET AL. 3 of 23



Jorgenson et al., 2001; Walters et al., 1998). Deep boreholes found permafrost at depths ranging from 7.3 m (Ferrick et al., 2008) to 47 m (Jorgenson et al., 2001), while electrical resistivity tomography indicated minimum thicknesses of >20 m were common (Douglas et al., 2015). Active-layer thickness above permafrost typically ranges from 50 to 75 cm in birch and spruce forests (Brown et al., 2015).

Groundwater upwelling sourced from the Alaska Range supports the nutrient-rich fens on the Tanana Flats (Ferrick et al., 2008; Racine & Walters, 1994). The linear fen complexes can stretch for tens of kilometers along linear channels that gently slope northward with empty into the Tanana River (Figure 1). Most of fens are concentrated in the Willow Creek Lowlands downslope of a large glaciofluvial outwash fan within the Wood River Uplands. While the Tanana Flats has an unusually high concentration of fens, they are similar ecologically to other fens we have studied in central Alaska (Jorgenson et al., 2013). The Tanana River (~115,500 km² watershed) is the largest tributary of the Yukon River, providing 20% of streamflow and 27% of groundwater to the Yukon River system (Walvoord & Striegl, 2007).

The vegetation is a highly patchy mosaic of birch and black spruce woodlands, dwarf birch and scrub, herbaceous fens and sphagnum bogs due to the variable near-surface mineral substrate, local hydrology, permafrost dynamics, and fire (Balser, 1996; Brown et al., 2015; Jorgenson et al., 1999, 2001; Lara et al., 2015; Racine, Jorgenson, et al., 1998). The collapse-scar bogs and fens are surrounded by permafrost plateaus associated with the lowland forests (Brown et al., 2015; Douglas et al., 2015; Jorgenson et al., 2001).

3. Methods

3.1. Study Design

As the data were compiled from numerous projects conducted from 1994 to 2016 there was no consistent study design across projects. The new remote sensing of fen changes used a systematic sampling approach to compare fen widths among three independent fens. The vegetation and soils data for the fens were compiled from an airboat disturbance and fen recovery project (Jorgenson, Murphy, et al., 2007), which used a gradient-oriented design that sampled at varying distances along six transects oriented perpendicular to the collapsing forest margin. The permafrost soils data for forests were compiled from an ecological land survey (Jorgenson et al., 1999, 2001) and a fire-thermokarst study (Brown et al., 2015; Douglas et al., 2015), which both used a gradient-oriented design to sample along transects that crossed permafrost and thermokarst terrain of differing ages. The new hydrology data reported here were collected using dataloggers positioned at three distances along a gradient from the outlets along the Tanana River to the head of the fen, and replicated across two fens. Locations of all sites used in this data set are provided in Table S1 in the supporting information.

3.2. Remote Sensing of Fen Changes

We developed a time series of georectified historical air photos and recent high-resolution satellite imagery to quantify areal changes in fens on the Tanana Flats using ArcMap. We identified three fen systems on the central portion of the Tanana Flats and digitized a center line through the fens based on the 1978 imagery (Figure 2). We subdivided the fens into a wider lower part and a narrower upper part with the hypothesis that lateral fen degradation may be more rapid in the wider, lower portions of the fens presumably caused by higher groundwater flow. For systematic measurement of fen widths we subdivided the center lines of the three fens into either 400- or 600-m segments depending on fen length to provide similar sample sizes (n = 25 to 35). Fen widths were then measured at the end of each segment. For each time period and sampling location we drew a line perpendicular to the centerline extending from western margin of the fen to the eastern margin. Fen margins were interpreted from the imagery and in most cases were distinctly evident as a sharp boundary between birch or spruce forest (individual trees were evident on the high-resolution imagery) and the herbaceous fen. In some cases, we differentiated low scrub on permafrost plateaus from fens. Occasionally, the margins were patchy and transitional; in these situations we visually interpolated an outer margin across discontinuous permafrost patches. Also, in some cases the 1949 air photos were of such low quality that a reliable interpretation was not possible; in these situations we assigned the 1949 margin to be the same as the 1978 position, leading to a slight underestimation of the change from 1949 to 1978. The line segments were attributed with year, fen number (1-3), fen size (L, S), segment, and point ID (PtID, concatenated fen number, segment number, and year). We also noted whether there were forested

JORGENSON ET AL. 4 of 23

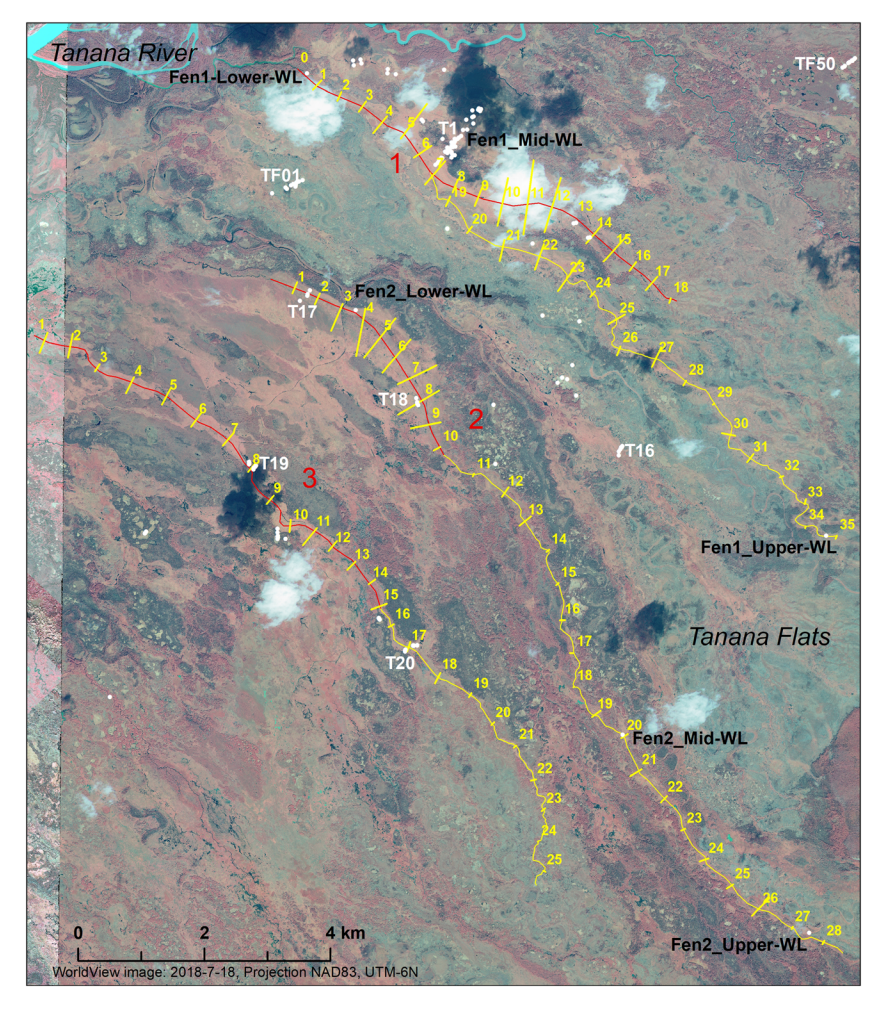


Figure 2. Map of centerlines (red for wide, yellow for narrow) and fen width measurement locations (yellow) for three fen systems on the Tanana Flats. Water-level stations (black) and main fen sampling transects (white) are also labeled.

islands present within the fens and if permafrost aggradation had occurred as indicated by newly developed permafrost plateaus within the fen system. We interpreted rapid transition from fens to birch forests to be a conclusive indicator of permafrost aggradation because the floating fen mats are too loose and submersible to support trees.

For the image analysis we obtained scanned images of black and white air photos (1.3 m pixel resolution) from August 1949 and color-infrared air photos (1.7 m) from 7/11/1978 from the EarthExplorer web server maintained by the U.S. Geological Survey (https://earthexplorer.usgs.gov/). A black and white orthophotomosaic (1.0 m) produced by AeroMap for U.S. Army Alaska in 1999 was used as the base map for georectifying imagery from other periods. High-resolution satellite imagery included a pansharpened IKONOS image (1.0 m) from 21 August 2003 and a pansharpened WorldView3 image (0.38 m) from 18 July 2018. We georectified the images to the 1999 orthophoto mosaic using ArcMap using distinctive features evident on the 1999 imagery as ground control points (usually ~20 points). The imagery was then rectified to the base images using second-order polynomial transformations, with rms errors ranging from 0.5 to 1.8 m. Coregistration errors were not a factor in the analysis, however, because the analysis depended solely on width measurements. The effects of varying spatial resolution (0.38–1.7 m) also was negligible because the resolutions differences were small relative to the overall change in mean fen widths (49.3 m) over the entire period.

For analysis, we calculated mean fen width by fen number, fen size, and year. The area of each fen was calculated by multiplying length by mean fen width. Significance of differences in mean fen width among fen

JORGENSON ET AL. 5 of 23



system and year were tested using a repeated measures ANOVA with the PtID as subject variable (repeated measurements at each point) and year and fen as fixed-factor variables.

3.3. Stratigraphic Indicators of Past Permafrost Degradation

We compiled data from previous studies (Brown et al., 2015; Jorgenson et al., 1999, 2001) with the main purpose of evaluating soil stratigraphy, ground ice content and morphology, identifying plant macrofossil indicators of environmental history, and evaluating stratigraphic ages. Soils sampling is briefly summarized here. For unfrozen surface soils, a soil plug (~40 cm diameter) was extracted with a shovel and a cross section was cut with a knife. Frozen soils were cored to 3–4-m depths using a 7.5-cm-diameter SIPRE (Snow, Ice, and Permafrost Research Establishment) corer. Soil stratigraphy was described according to Natural Resources Conservation Service methods. Cryostructures were described using the system of French and Shur (2010). Samples were obtained every ~20 cm and analyzed for bulk density, volumetric moisture, pH, electrical conductivity (EC), and total organic carbon.

Several samples were collected at distinctive breaks in peat stratigraphy for radiocarbon dating. Samples collected in 1994 and 2003–2005 were analyzed at Beta Analytic (Miami, FL) by standard radiometric methods and samples from 2012–2013 were analyzed by accelerator mass spectrometry at the National Ocean Sciences Accelerator Mass Spectrometry Facility (Woods Hole, MA). Ages were reported as conventional radiocarbon dates. For samples with modern conventional dates (<120 yr old), we assigned a maximum calibrated age date of 200 yr, based on the maximum limit of the 2-sigma age range.

3.4. Ecological Succession

To assess early successional development of fens, using data primarily from Jorgenson, Murphy, et al. (2007), changes in vegetation, hydrology, and soil were determined along six toposequences running from the thermokarst "moat" at the edge of the fen (early succession) to the center of the fen or to shrub fens (late succession) (Figure 2). Along each toposequence, a single plot $(4 \times 10 \text{ m})$ was established in subjectively identified zones that had distinct differences in fen vegetation, for a total of 37 plots (T-series). In addition, 18 plots from the airboat disturbance study that were used as undisturbed reference plots (R-series) were included in the data set.

At each plot, measurements were made of vegetation, water, and soil properties. Monitoring locations were accessed by helicopter during mid-July 2003–2005. Plant cover was determined by point-sampling at 100 points (including repetitive "hits" for all layers) distributed along five equally spaced rows (4-m long, 20 points per row) across the 10-m-long plot. The plots were examined for additional species and a cover of 0.1% was assigned to all species not captured in the point sampling. Taxonomy follows that of the Flora of Alaska provisional checklist (https://floraofalaska.org/provisional-checklist/). To relate cover estimates to biomass, additional vegetation and biomass sampling were done at a subset of 15 plots. Within each plot, one small quadrat (0.5 m^2) was sampled for vegetation cover with a point frame and then clipped. Plants were sorted by species. Regression equations were developed to relate cover to biomass.

Environmental properties were measured at each plot, including parameters for water, soil, and age. Water depth above (+) or below (-) the mat surface was measured with a ruler and soil probe, and pH and EC were measured with Oakton portable meters (meter calibration was checked daily and recalibrated with three standard solutions as needed). Soil sampling was done at each plot to determine organic mat thickness, total dry weight, and organic carbon content. Two samples of the entire floating mat at each site were obtained using a 3-in diameter corer. One sample was for determining root biomass and the second for determination of total dry weight and organic carbon content. The organic carbon content was determined by a LECO TNC analyzer after the samples were air dried and the entire sample was ground. Time since disturbance (thermokarst) was estimated from thermokarst rates determined from 1955 and 1999 photography. At the oldest plot at two of the chronosequences, a sample was obtained from the base of the mat (or from birch bark at the top of the submerged forest peat) and analyzed for radiocarbon age (described above). Basal organic samples were not taken from the other three transects because birch bark from dead trees underneath the mat could not be found.

Plant associations were developed from the plot data in a three-step process. First, two-way indicator species analysis (Twinspan, PCord, MjM Software Design, Corvallis, OR) provided the initial sorting of species by plot. Second, plot groupings were evaluated using nonmetric multidimensional scaling (NMDS), a

JORGENSON ET AL. 6 of 23



multivariate ordination technique, using PC-ORD 7 (MjM Software, Gleneden Beach, OR). Third, inconsistencies between groups identified from Twinspan as plotted using the NMDS output were identified and additional manual sorting was done to adjust the classification of a few plots based primarily on the structure of the dominant species. The plant associations were then named based on the dominant species and an indicator species that helps differentiate between similar classes.

3.5. Hydrology

Water levels and temperatures of near-surface groundwater at two parallel, 15-km-long fens (three sites each) and a small lake (Figure 2) were measured hourly from summer 2011 through early fall 2014 using nonvented pressure transducers (HOBO U20 Fresh Water Level Data Logger 13 ft, U20–001-04, Onset Hobo Company, Bourne, Massachusetts). They were deployed inside a 4-cm-diameter perforated PVC pipe situated at least 10 m from the fen margin. The sensors rested on top of a 1-cm-diameter steel rod with a 3-cm-diameter cap. The rod was pounded into the sediments below the floating mat with a slide hammer to a depth greater than the typical seasonal freeze-thaw depth in the area (usually 1.5 m) to avoid jacking from seasonal frost. The sensors were between 1 and 1.5 m below the water level in the fall and secured to the top of the pipe with a slacked line for retrieval. Barometric pressure measurements were made using an additional sensor hung from a tree at the Lake, Fen 1_Mid, and Fen 2_Upper sites (Figure 2). Elevations of the sensors were determined using a high-resolution, differential global positioning system (DGPS). Based on the measurement error for the z coordinate direction with the DGPS and the pressure transducer (\pm 0.3 cm of water) we estimate the vertical water level elevation error to be \pm 4 cm. Wells were accessed via helicopter (summer) or snow machine (winter) for downloading and maintenance.

For data processing and analysis, we used HoboWare (Onset Computer Corporation, Bourne, Massachusetts) for initial processing and barometric pressure correction and the data were compiled into an Excel database. To allow comparison of water-level trends among sites, the long-term mean water surface elevation (WSE) of each site (ranging from 128.48 to 162.58 m amsl) was subtracted from the hourly readings to provide a normalized stage (above and below average reference height). Mean daily water levels and temperatures were calculated and plotted to examine temporal trends.

3.6. Climate

Climate records for Fairbanks (UAF Experiment Station) from 1904 to 2019 were acquired from the National Oceanic and Atmospheric Administration (https://www.ncdc.noaa.gov/cdo-web/). Additional data were obtained for the Nenana station (about 70 km southwest of Fairbanks), to fill in small data gaps (particularly precipitation/snow depth ruler measurements) in the Fairbanks record. We attributed the data with fields for summer (May–September, MJJAS) and cold winter periods (November–March, NDJFM) and hydrologic year (October–September) and calculated mean air temperature and snow depth on the ground by seasonal period (average of daily values) and year. Cumulative precipitation (sum of daily values) was calculated for the summer. The broad summer and winter periods were of interest because warmer and wetter summers increase soil heat input and warmer and snowier winters reduce soil heat loss.

In evaluating climate extremes there are a wide range of definitions that variously include high impact events, exceedance thresholds of temperature and precipitation, rare events with a long return period (e.g., 50-yr return period), and "unprecedented" events (Field et al., 2012). Here we used exceedance thresholds (10th and 90th percentile) to identify unusual, or "extreme" years. To identify years of unusual thermal effects seasonal mean temperature, cumulative precipitation, and mean snow depth were calculated and plotted. The main axis of the temperature-precipitation gradient was defined by the mean and \pm SD of long-term air temperature and precipitation records. Lines perpendicular to the trendline (defined by opposing +1 SD and -1 SD values) were used to identify the top 10% of the extreme years at both ends of the gradient. While the effects of temperature and precipitation on soil heat flux are not linear, this generalized gradient is sufficiently robust to identify years with unusual thermophysical effects.

4. Results

4.1. Remote Sensing of Recent Fen Changes

The remote sensing of fen changes at 88 cross sections systematically distributed across three fens, based on a time series of high-resolution imagery from 1949 to 2018, revealed that the fen systems were highly variable

JORGENSON ET AL. 7 of 23

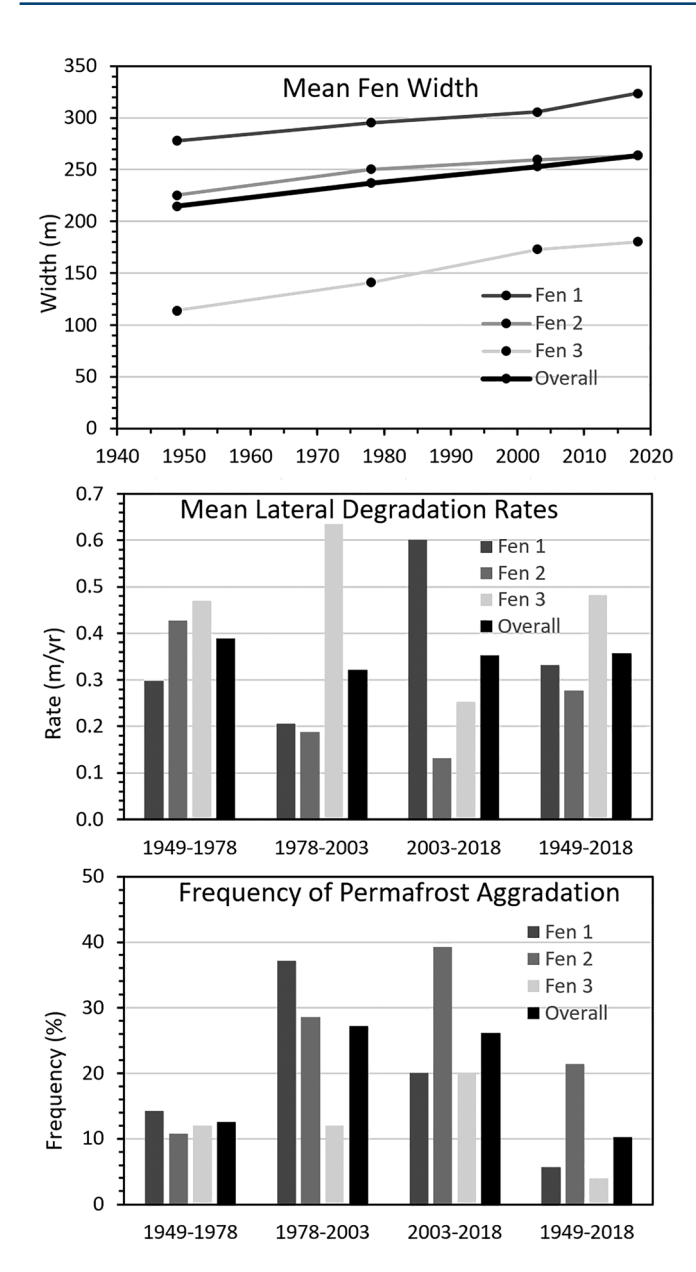


Figure 3. Changes in (top) width, (middle) lateral degradation rates, and (bottom) frequency of permafrost aggradation during three time periods from 1949 to 2018 for fen systems on the Tanana Flats, Alaska. For the overall period, frequency of permafrost aggradation was much less than during individual periods because lateral losses during degradation periods usually were much larger than gains during aggradation.

spatially and highly dynamic over three time periods (1949–1978, 1978–2003, 2003–2018). The repeated measures analysis found that mean widths significantly (p=0.04) varied twofold among the three fens (Figure 3). Overall, mean fen widths increased from 214.6 m in 1949 to 263.9 m in 2018, but the differences among periods were not significant (p=0.20) due to the high variability among cross sections. Total area (lengths times average width) of the three fens increased 23% from 9.9 km² in 1949 to 12.2 km² in 2018.

When calculated as a lateral rate of permafrost degradation per year for each margin, the overall lateral degradation rate at the margins of the three fens was 0.36 m/yr over the 69 yr, and ranged from 0.32 to 0.39 m/yr across the three periods. When comparing among fens, rates varied from 0.28 to 0.48 m/yr (Figure 3). Mean rates showed different patterns for each fen over time: for Fen 1 rates decreased during the second period relative to the first period and then increased during the third period; for Fen 2 rates decreased every period; and for Fen 3 rates increased and then decreased. Mean rates by fen and period varied fivefold from 0.13 to 0.64 m/yr.

Permafrost aggradation was observed in every fen system and in every period. Overall, permafrost aggraded at old stabilized margins or in the centers of 10% of the 88 cross sections across all fens during the 69 years (Figure 3). Averaged over the entire period, permafrost aggradation was fourfold more frequent in Fen 2 compared to the other fens. When comparing individual fens over time, aggradation frequency at Fen 1 increased then decreased, at Fen 2 consistently increased, and at Fen 3 stayed the same during the first two periods and then increased. When comparing the overall frequency for all fens among periods, aggradation was observed at 13% of the cross sections during 1949-1978, 27% during 1978-2003, and 26% during 2003-2018. An example of island aggradation and degradation is presented in Figure 4, where no forested islands were present in 1949, initial aggradation was evident in 1978, and a well-developed birch island on a new permafrost plateau had developed by 2003. However, by 2018 much of the island had degraded. Field observations at a few locations in 2001 and 2004 showed heaving of the ground surface and death of hydrophytic vegetation that we attributed to permafrost aggradation, although direct observations of permafrost characteristics through coring were not made. We conclude the permafrost aggradation occurred shortly before these observations (Figure 5).

4.2. Stratigraphic Indicators of Past Permafrost Degradation

From the compilation of soils data from 21 permafrost cores we identified five cores that had a buried herbaceous peat layer with plant macrofossils (*Menyanthes trifoliata*, *Equisetum fluviatile*) indicative of fens that devel-

oped after a previous thermokarst episode (Figure 6). This herb peat ranged from 3 to 13 cm thick and at depths of 17 to 32 cm. Woody forest peat was found above the herb peat. Below the herb peat were thick layers of moderately decomposed mucky peat and cryoturbated mixtures of silt and mucky peat, indicating deformation of soils from thermokarst. All sites with buried herb peat were associated with birch forests, whereas herb peat was not evident at four birch forest sites and at all 15 black spruce sites (including burned black spruce). All sites were underlain by fluvial interbedded silt and sand, with one silt having a basal gravel layer. Radiocarbon dating of peat below the fen peat ranged from 1,550 to 5,330 ¹⁴C yr BP.

Cryostructure descriptions of the five permafrost cores in birch forests indicate the permafrost was ice-rich (visible excess ice >40%) to maximum depths ranging from 3 to 3.5 m. The ice-rich layers typically were associated with organic-matrix, layered, braided, reticulate, and ataxitic cryostructures. Of particular interest

JORGENSON ET AL. 8 of 23

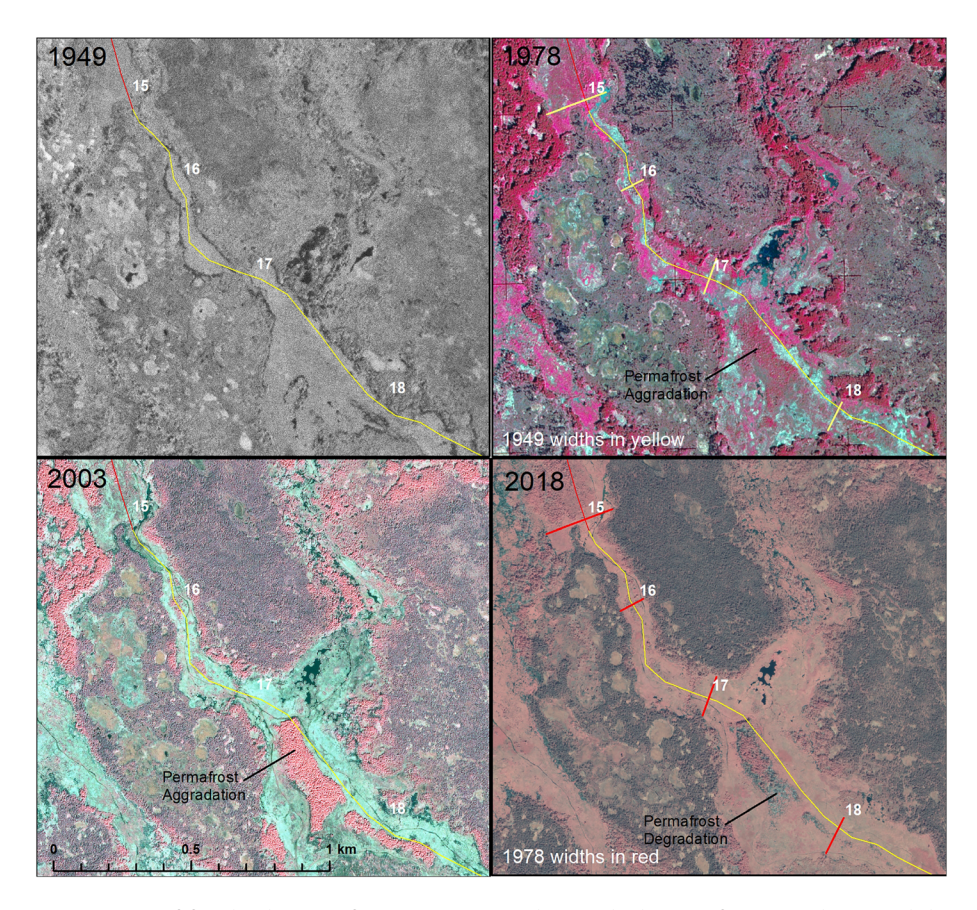


Figure 4. Time series of fen development from 1949 to 2018 showing both permafrost aggradation and degradation within fen systems, Tanana Flats, Alaska.

was the frequent occurrence of thick sequences of layer ice (bedded), with individual ice layers often 2–3 cm thick. We interpret the permafrost to be epigenetic permafrost formed by downward aggradation after refreezing post thermokarst.

Herb peat was observed at 82 soil profiles in fens where no permafrost was observed. Representative profiles from midsuccession fen stages are presented in Figure 6. For this intermediate stage, herb peat thickness ranged from 28 to 80 cm. Woody peat, frequently with birch bark present, and indicative of collapsed forest was found at nearly all sites (at some sites we did not record observations below the fen peat). Radiocarbon dating of birch bark from the top of the woody peat layer indicated all samples were modern (range 50 to 102 ¹⁴C yr BP).

4.3. Ecological Succession

Vegetation, soils, water chemistry, and age in the fens exhibited large changes associated with ecological succession after permafrost degradation and forest collapse (see Figure 5, e.g., of successional gradients from collapsing forest margins to fen centers). Floristic analysis of the plant species composition in 54 plots differentiated six plant communities (named after their dominant and differential plant species): Calla palustris-Bidens cernua (hereafter Bidens using only the dominant species), Calla palustris-Carex aquatilis (Arum, using common name), Carex aquatilis-Lemna turionifera (Sedge), Menyanthes trifoliata-Equisetum fluviatile (Buckbean), Comarum palustre-Equisetum fluviatile (Cinquefoil), and Betula nana-Salix bebbiana (Birch-Willow) (Figures 7 and S1 and Table 1). For environmental analysis, the Bidens type was lumped with the Arum type due to their occurrence immediately adjacent to the collapsing forest margin, their dominance by Calla palustris, and to increase sample size. A few plots were strong outliers in the NMDS ordination in terms of their species composition (Figure 6), but were maintained with their final class for environmental analysis (one was a distal plot with abundant willow but lacking in dwarf birch, and one

JORGENSON ET AL. 9 of 23



Figure 5. Photos of permafrost degradation along the forest margin (upper left), the successional gradient from the margin to the center (upper right), and photos of surface heaving and dead vegetation caused by permafrost aggradation soon before (lower left) 2001 to (lower right) 2004.

was at a collapsing edge with abundant water but lacking in *Calla palustris* because it was too young for *Calla* to colonize).

Plant cover (repetitive cover representing all hits across multiple layers) showed large differences in species composition between the early-successional Arum type and the late successional Birch-Willow type (Table 1). The composition of the midsuccessional Buckbean and Cinquefoil types, however, was predominantly the same, varying mostly in the relative cover of the dominant species. *Menyanthes trifoliata*, *Comarum palustris*, and *Carex aquatilis* were the most abundant species, and present in all vegetation types.

Total mean biomass varied little (range 0.35 to 0.42 kg/m²) among four of the vegetation types (no data for the Sedge type), but there were large differences among lifeforms across the successional sequence (Figure 8). Forbs and sedges comprised all the biomass in the Arum type, forbs dominated the Buckbean and Cinquefoil types, and shrubs dominated the Birch-Willow type. Biomass was strongly related to the repetitive cover for both sedges ($R^2 = 0.63$ for *Carex aquatilis*) and forbs (R^2 ranged from 0.59 to 0.88; Figure 8).

Mean water depths varied fourfold among vegetation types, ranging from $32 \, \mathrm{cm}$ in the Arum type to $-10 \, \mathrm{cm}$ (below the surface) in the Birch-Willow type with confidence intervals showing no overlap between early and late-successional stages (Figure 9). Mean water pH (loosely related to nutrient status) varied little across the successional stages. Mean EC (an indicator of groundwater input) varied twofold among types, was highest in the Buckbean type, and trended lower during middle-late succession.

Soil properties showed large differences across the successional sequence (Figure 9). Mean thickness of herb and sedge peat formed following thermokarst varied threefold among types, increasing from 18.5 cm in the Arum type to 70.3 cm in the Birch-Willow type. Mean bulk density (whole core) of postthermokarst peat varied fourfold among types, increasing from 0.02 g/cm³ in the Arum type to 0.09 g/cm³ in the Birch-Willow type. The mean carbon stock varied tenfold among types, increasing from 1.5 to 16.4 kg/m² in the Birch-Willow type, as a result of the combined effects of both increasing thickness and density. The overall long-term rate of soil carbon accumulation was $60 \, \text{g/m}^2/\text{yr}$, based on total carbon stock and estimated age for the Birch-Willow stage. The increasing thickness and density also allowed the initial floating mat occurring in early succession to compress against the collapsed buried soil and elevate the surface above the water table during late succession.

JORGENSON ET AL. 10 of 23

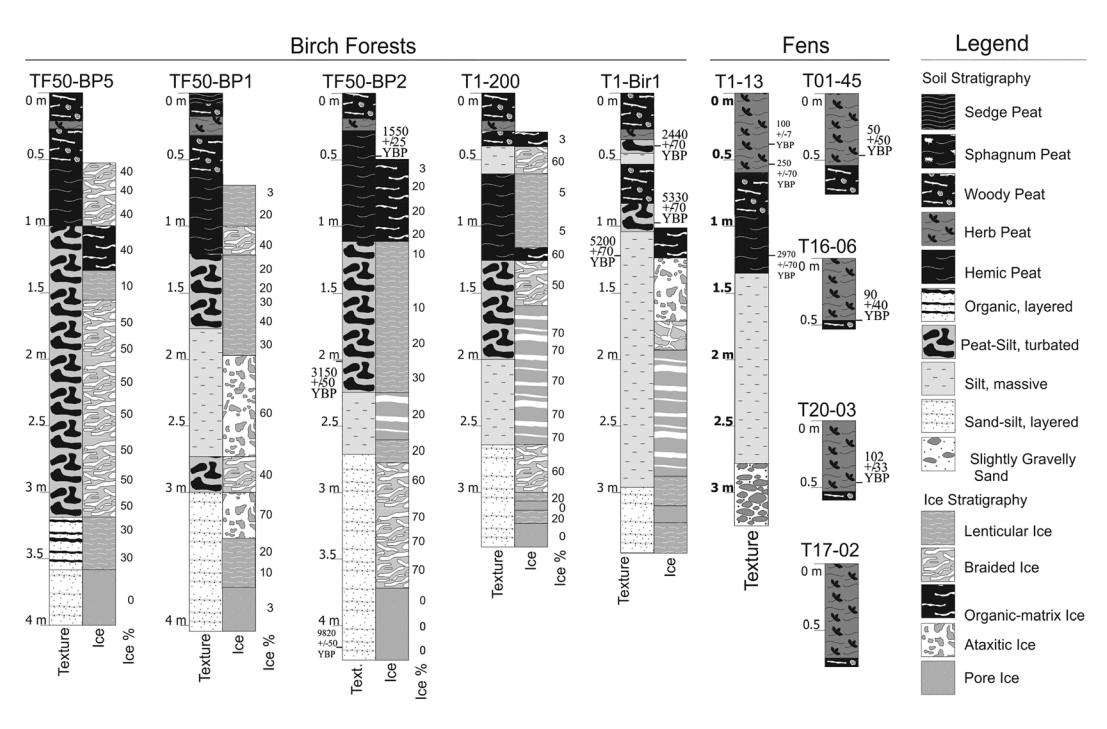


Figure 6. Soil and permafrost stratigraphy of representative cores, along with radiocarbon dating, for fens and birch forests that had fen peat layers indicative of past degradation and aggradation, Tanana Flats, Alaska.

The mean distance from the plots to the forest edge was used to calculate mean site age based on retreat rates calculated from the bank changes near the beginning of each transect using imagery from ~1949 to 1999

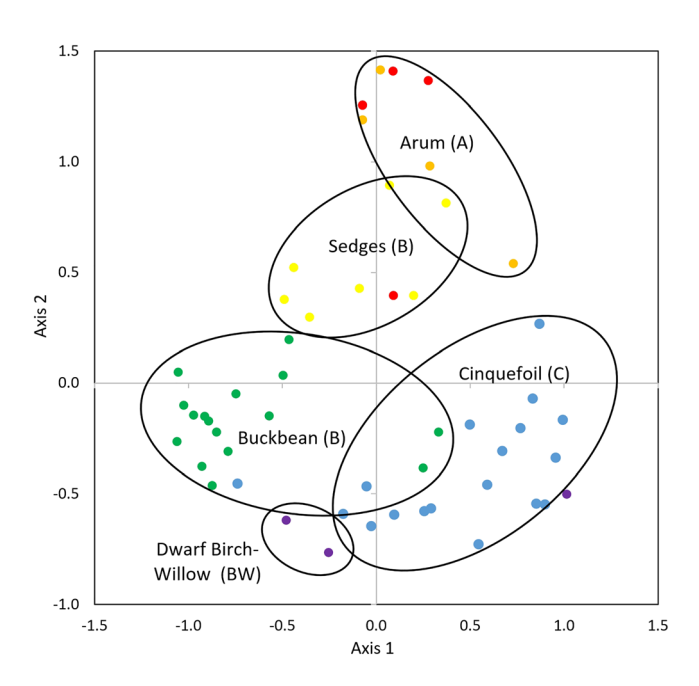


Figure 7. Ordination and classification of fen plant community composition based on nonmetric multidimensional scaling (NMS), Tanana Flats, Alaska. Ellipses identify central clusters, excluding a few outliers, and plant communities were denoted by their dominant species. Bidens type (red) was lumped with the arum type (orange) for environmental analyses.

(Figure 9). Mean distance increased from 8.7 m in the Arum type to 146 m in the Birch-Willow type. Mean age was estimated to increase from 17.5 yr in the Arum type to 250 yr in the Birch-Willow type, with no overlap in confidence intervals among most types.

4.4. Hydrologic Regimes

4.4.1. Water Levels

Water levels at varying distances along two fens, and a headwater lake, showed large differences in stage among sites and seasonally (Figure 10). The largest water-level fluctuations across all years were observed at the lake site, which varied by 2.49 m. In fens, the largest ranges occurred at Fen 2_Mid (1.44 m) and Fen 2_Upper (1.30 m), while the smallest range occurred in Fen 1_lower (0.64 m).

Seasonal trends in water levels showed that all sites had large, abrupt increases in water level during spring snowmelt (ranging from 0.5 to 1.1 m in the fens), followed by a rapid decline of 0.2 to 0.4 m over a period of 1 to 2 weeks. The persistent increase in water levels during snowmelt indicates most of the surface melt moves subsurface to recharge the subsurface water in the floating mat, while only a small portion of it runs off. During summer, there was a consistent slow decrease in water levels of 0.1 to 0.2 m until August. During fall and early winter, the water levels typically held mostly steady or even increased slightly until December, even though precipitation was locked in snow and the surface had started to freeze downward. From about December until snowmelt in April most sites had gradual and consistent drawn-downs.

When comparing differences in water levels among sites, there was a remarkable contrast in hydrologic regimes among sites, particularly

JORGENSON ET AL. 11 of 23



Table 1Mean Percent Cover (Multilayered, Totals >100) of Common Plant Species in Fens by Plant Community Type

Plant species	Callpal-Bidcern	Callpal-Caraqu	Caraqu-Lemtur	Mentri-Equflu	Compal-Equflu	Betnan-Salbeb
Sparganium angustifolium	1					
Bidens cernua	1					
Myriophyllum sp.	$\frac{1}{4}$	0			0	
Carex canescens	2	2				
Calla palustris	43	41		0		
Lemna turionifera	18	11	1	1		
Calamagrostis canadensis	3	0	$\frac{1}{0}$		0	4
Hippuris vulgaris	1	0	1	0	0	0
Ranunculus gmelini		1				
Lysimachia thyrsiflora		1	0	2		
Typha latifolia		2	3	1	0	
Carex utriculata	7	34		3	2	
Utricularia intermedia	3	1		8	0	5
Cicuta virosa	2	2	1	2	1	
Carex aquatilis	1	76	64	13	9	1
Menyanthes trifoliata	1	4	22	136	29	31
Comarum palustris	1	15	8	8	66	31
Galium trifidum	-	1	1	2	2	1
Equisetum fluviatile		-	0	<u>6</u>	17	11
Epilobium palustre		1	1	<u>×</u> 1	1	1
Unknown mosses		0	3	1	12	31
Carex diandra		· ·	, and the second	2	8	10
Mnium sp.			0	2	2	5
Calamagrostis inexpansa			4	0	1	2
Myrica gale			7	1	-	5
Calliergon sp.		0	,	1	6	10
Carex chordorrhiza		· ·		1	3	10
Alnus incana tenuifolia			0	0	, and the second	
Stellaria sp.			0	1	0	0
Salix candida			· ·	3	0	2
Rumex arcticus				0	0	-
Carex limosa				Ü	1	
Petasites sagittatus					0	1
Eriophorum gracile					0	1
Scutellaria galericulata					Ü	0
Salix pulchra		1		0		1
Salix arbusculoides	0	1		0		2
Betula neoalaskana	U	0		0	0	2
Pedicularis parviflora		O		O	1	1
Salix bebbiana				0	1	6
Parnassia palustris				U		<u>9</u> 1
Betula nana						11
Litter	3	4	12	4	15	$\frac{11}{10}$
Bare soil	3 1	4	12	4 1	15	10
Water	93	90	19	55	3	15
		89				15
Sample size	4	4	7	16	19	3

Note. Values (rounded whole number, blank when absent) are underlined for dominant and differential species used for community name (abbreviated for header), bolded when associated frequency threshold (not presented) >50%. Other trace species are as follows: Agrostis scabra, Symphyotrichum falcatum, Drepanocladus sp., Drosera anglica, Glyceria maxima, Rhizomnium sp., Spiranthes romanzoffiana, and Triglochin maritima.

during winter. The Fen1_Upper and Fen2_Mid had similar regimes that followed the main pattern described above. The Fen1_Mid and Fen2_Lower differed substantially, however, in that they had very small winter drawdowns of <0.2 m, while at Fen2_Lower the water levels increased throughout the winter of 2012–2013. We attribute the simultaneous decrease in upper fens and increase in lower fens in late winter to continuing subsurface flow of water from upper fens (elevations 136–142 m) to lower fens (elevations 128–129 m). The fall and early winter recharge in the upper fens also indicates groundwater recharge is seasonal, with subsurface flow into the systems increasing during fall and tapering off during late winter.

JORGENSON ET AL. 12 of 23

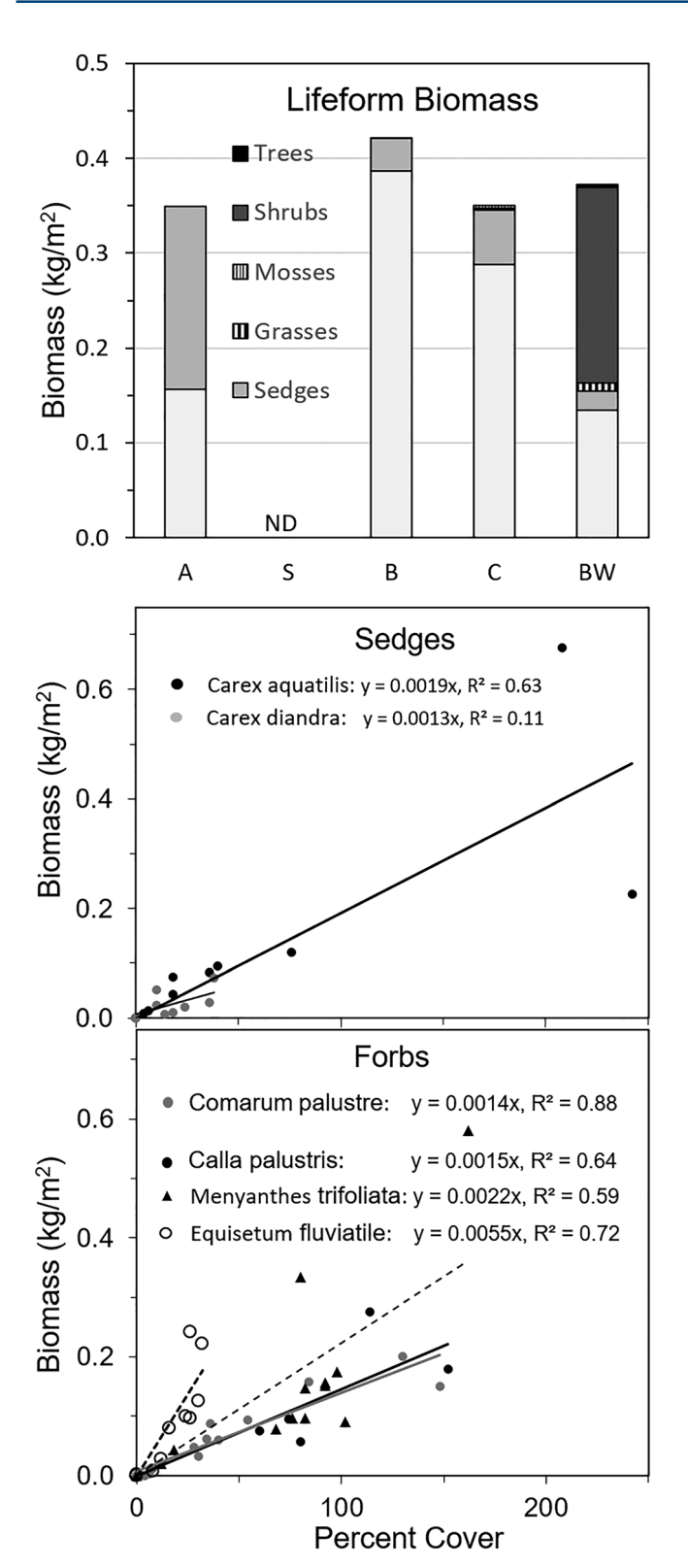


Figure 8. Mean total plant biomass (top), as well as by growth form, in the Arum (A), Buckbean (B), Cinquefoil (C), and Birch-Willow (BW) stages of fen succession, Tanana Flats, Alaska. Regression relationships of biomass to cover of major sedges (middle) and forbs (bottom) are also provided.

Based on these characteristics we attribute the source of the groundwater to be from the Wood River as it crosses the large fan of coarse glaciofluvial outwash deposits in the southwestern portion of the Tanana Flats. This fan is apparent on the Landsat image in Figure 1 and most fens are situated immediately below this glaciofluvial outwash. In the imagery the drainage patterns on the outwash fan extend from the Wood River to the middle portion of the western Tanana Flats, whereas, in the eastern portion of the Flats the surface drainage patterns primarily are associated with paleochannels of the Tanana River, and to a lesser extent Dry Creek. There are few fens in the eastern portion of the Flats. This indicates watering flow in the Wood River, which peaks during mid-summer glacial melt, recharges the aquifer in the glacial outwash during middle—late summer and provides groundwater for recharging the fens during early winter.

High-precipitation events lasting multiple days during summer had relatively small but distinct effects on water levels (Figure 11). Eleven high-precipitation (cumulative amount >20 mm at Fairbanks) events were observed during 2012-2014, varying from 1 to 12 days in length and from 19 to 91 mm in cumulative precipitation. Of particular interest, total precipitation (295 mm) during the summer (June-August) was the second highest on record over the 105-yr observation period for Fairbanks. Daily record precipitation events occurred on 1 July (49 mm), 1 August (23 mm), and 1 September (36 mm). At Fen1_Upper, where water levels were the most responsive to precipitation, water-level increases of 11 to 156 mm were observed during the events. Water-level increases during the events were highly correlated to cumulative precipitation ($R^2 = 0.74$), with water levels generally increasing at twice the amount (cm) of precipitation inputs. The other sites showed similar trends in water-level responses, but with the Lake typically showing larger responses and other fens slightly lower responses. Because the water surface is within a few centimeters of the floating mat surface, and the loose mat is highly porous, we attribute the response mostly to the immediate change from precipitation input and to the slower response over days to near-surface movement of water down the fen channels.

4.4.2. Water Temperatures

Water thermal regimes were evaluated in terms of overall differences among sites, seasonal trends common among all sites, and differences in seasonal trends among sites (Figure 10). Over the approximately two and a half year period, the mean temperature across all sites was 3.4°C and varied from 1.1°C at Fen1_Upper to 3.9°C at the Lake, while the other four sites only varied from 3.5°C to 3.6°C. For all sites grouped together, mean annual temperatures (hydrologic year) varied only slightly from 3.0°C in 2013 to 3.1°C in 2014 using only the two years with complete annual records. When comparing thawing-degree days (TDD, sum of mean daily temperatures) by hydrologic year (only complete years used), TDD varied from 396 at Fen1_Upper to 1,405 at the Lake, while the other four sites only varied from 1,261 to 1,291. Maximum summer temperatures across all years varied from 4.3°C at Fen1_Upper to 13.3°C at the Lake, while the other four sites varied from 7.7°C to 11.2°C, minimum temperatures were near 0°C for all sites. We attribute the higher temperatures in the lake to radiation and mixing effects, while the unusually low temperatures at Fen1_Upper is not readily explainable, perhaps due to different soils (pipe and sensor within mineral soil) or the location of the site in a small fen tributary away from the main channel.

JORGENSON ET AL.

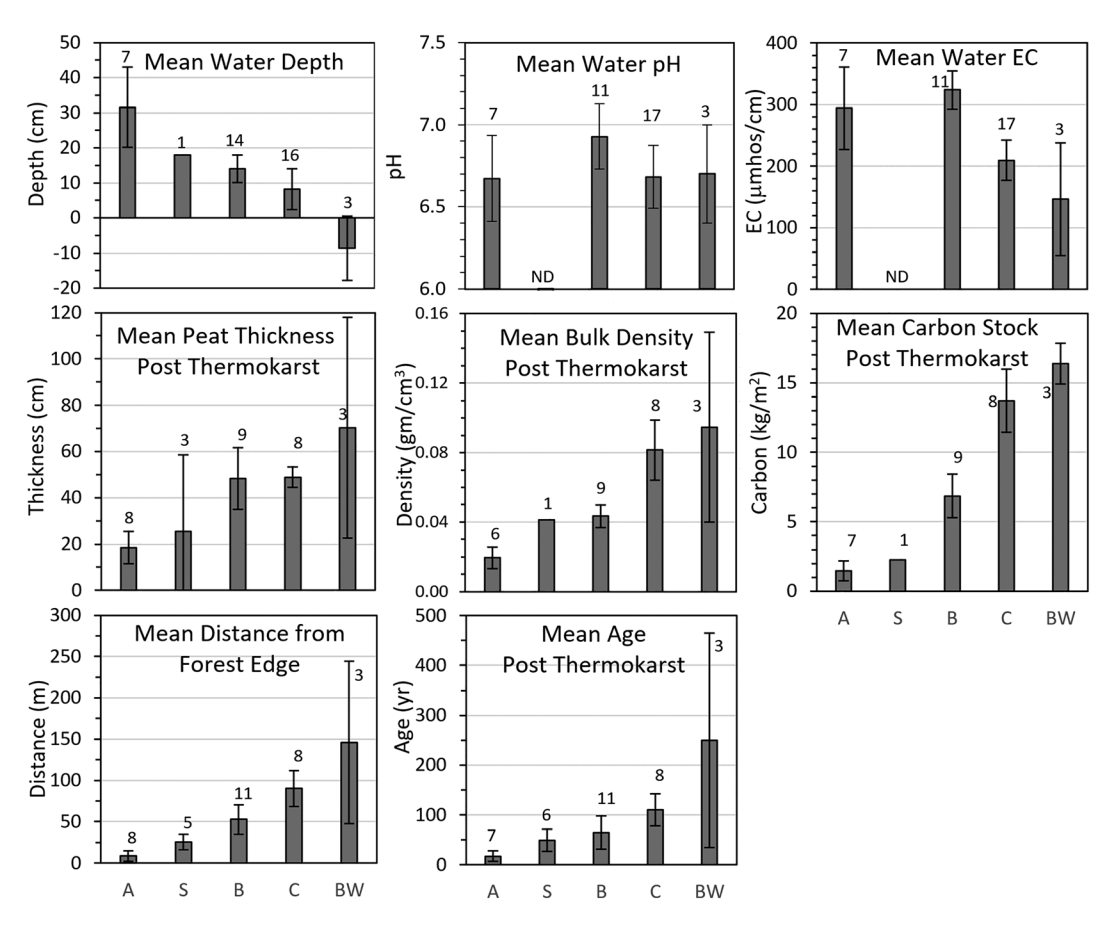


Figure 9. (top row) Mean (95% CI) depth, pH, and electrical conductivity (EC) of water, and (middle row) postthermokarst values for peat thickness, bulk density, and total organic carbon, as well as (bottom row) distance to forest edge and estimated age, in the Arum (A), Sedge (S), Buckbean (B), Cinquefoil (C), and Birch-Willow successional stages of fen ecosystems on the Tanana Flats, Alaska.

Seasonal patterns common to all sites were differentiated into spring thaw, early summer warming, late summer cooling, and winter freeze down. Spring thaw begins at snowmelt with temperatures remaining near 0°C and ends when the winter frozen layer completely thaws and temperatures start rising. Occasionally, there was a temperature spike at the onset of this period that we attribute to subsurface infiltration of meltwater. Early summer warming was associated with rapid warming from near zero in May to early June to maximum summer temperatures around early August. The beginning of this phase varied considerably among sites and years, however, due to variations in spring air temperatures and snowpack thickness. Late summer cooling was marked by rapid cooling from mid-August until surface freeze-up around late September to early October. Although there often were small spikes and dips in temperatures associated with this transition, it can be difficult to detect from deep subsurface temperatures alone. Finally, the winter freeze-down phase denotes slow, gradual cooling to near zero as the frozen layer thickened. At the Lake, the winter frost line probably extended down to the sensor because the pressure transducer produced erroneous values (shown as missing values in Figure 10) the winter of 2013, but after thawing we presume the sensor returned to accurate readings because water levels during snowmelt recharge were very similar among years.

When comparing differences among sites for the various seasons, a few notable differences stand out. First, differences were not always consistent. For example, Lake summer temperatures were ~3°C higher than most other sites in 2012 and 2013, but similar to the other sites in 2014. We attribute the lower summer temperatures in the Lake in 2014 to the numerous high-precipitation events and mixing. Fen2_Lower, however, showed the opposite trend. Second, Fen1_Upper, which had much lower overall temperatures than the other sites, also was unusual in that maximum summer temperatures occurred in September instead of August, as was typical of all other sites. We attribute the lower temperatures and persistent warming later

JORGENSON ET AL. 14 of 23

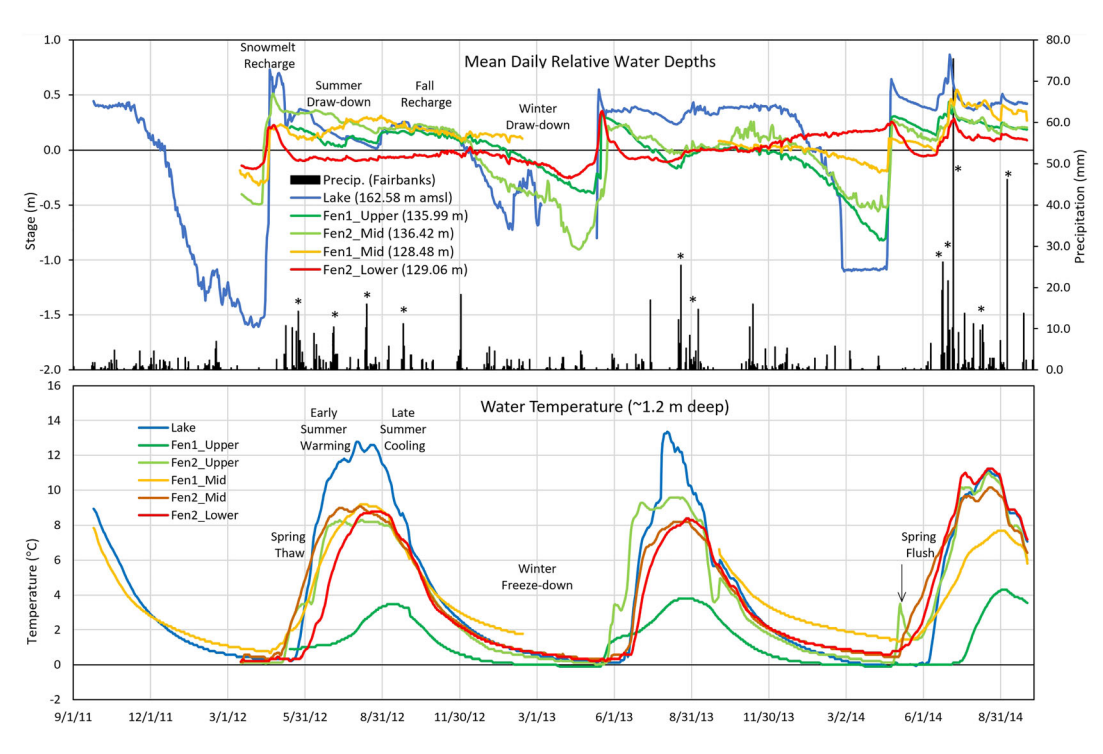


Figure 10. Mean daily water stage (relative to long-term mean, above) and temperatures (below) for three distances (upper, middle, lower) within two fens and at a groundwater-fed lake ~15 km south of the two fens. Daily precipitation (Fairbanks Airport) is also provided (above), with multiday, high-precipitation (cumulative >20 mm) events are marked with *.

into the fall to greater relative input of groundwater. Third, beginning and end of the spring thaw phase was highly variable across sites and years, indicating site-specific variations in snowmelt and groundwater input are important factors.

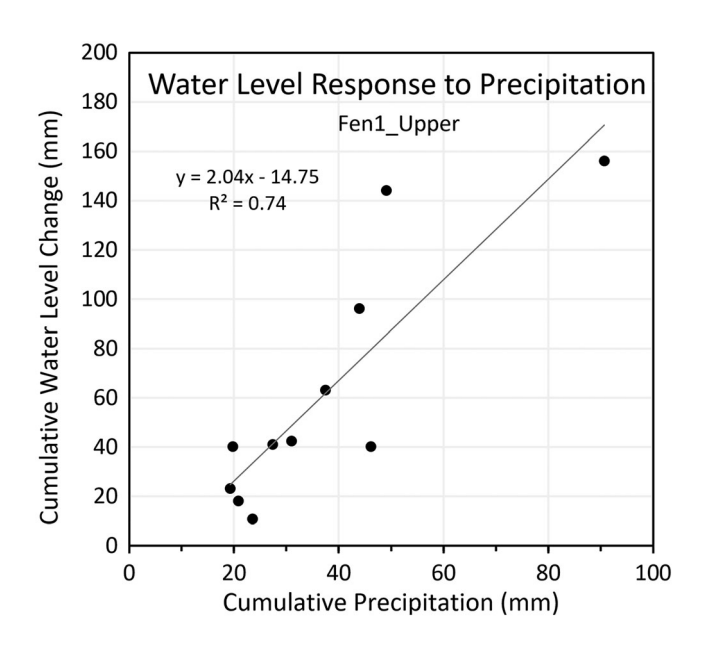


Figure 11. Short-term response of fen water-levels (cumulative increase over event period) to 11 major multiday precipitation events (>20 mm, Fairbanks station) during summers 2012–2014, Tanana Flats, Alaska.

4.5. Climate Change and Extreme Events

Climate records for Fairbanks from 1904 to 2019 were used to identify periods of extreme (<10th and >90th percentiles) summer (May–September) temperatures and precipitation, and winter (November-March) temperatures and snow depths that were favorable to permafrost aggradation and degradation (Figure 12). Of particular interest for permafrost degradation are warmer and wetter summers that increase soil heat input, and warmer and snowier winters that reduce soil heat loss. Cold, less snowier winters are particularly favorable to soil heat loss and permafrost aggradation. Overall, the range in mean winter air temperatures $(-11.8 \text{ to } -23.7^{\circ}\text{C})$ was 3 times larger than that for mean summer air temperatures (10.0-13.8°C), while cumulative summer rainfall ranged fourfold (88.6–384.6 mm) and winter snow depths (daily values of depth on ground averaged over winter period) ranged sevenfold (10.9-79.7 cm). On an annual basis, mean annual air temperatures ranged from −5.7 to 1.0°C (average -2.4°C) and mean annual cumulative precipitation ranged from 114 to 685 mm (average 303 mm).

Overall, there was a distinct trend in summers becoming warmer and wetter over time, with the 2010s having 3 years in the top 10% and three other years just below the 10% threshold (Figure 12). Decades with more frequent warm, wet summers or warm, snowier winters favorable for permafrost degradation include the 1980s (three occurrences of either) and the

JORGENSON ET AL. 15 of 23

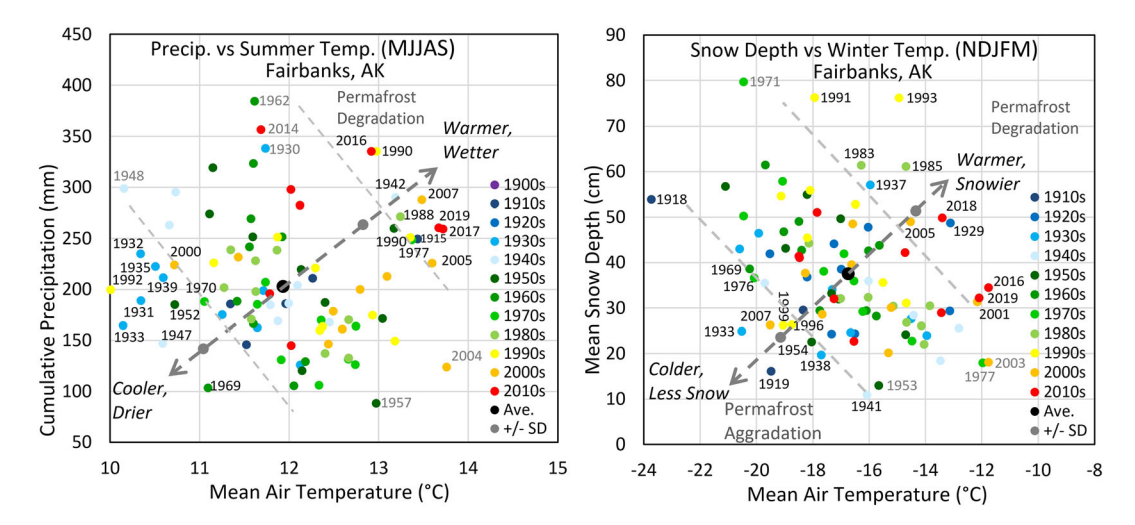


Figure 12. Plots of mean cumulative summer (MJJAS) precipitation (PR) versus air temperature (AT, left) and average winter (NDJFM) snow depths on the ground and AT (right). The values are color coded by decade, including overall averages (black dot) and ± 1 standard deviation (SD) from the mean (gray dot). The dark dashed line bisects the SDs of the PR and AT values and represents the warmer-wetter and cooler-dried gradient, while the light gray dashed line (perpendicular to gradient) demarks the 10% most extreme years at the ends of gradient. Extreme years at the ends of the gradient are labeled in black, while extremes for only one condition are in gray. Both unusually warm and wet summers, and warmer and snowier winters, make permafrost vulnerable to degradation, while colder and less snowier conditions facilitate permafrost aggradation.

2010s (seven). Decades with more frequent cool, dry summers or cold, less snowy winters include the 1930s (seven) and 1990s (three).

5. Discussion

5.1. Permafrost Aggradation and Degradation

The remote sensing of fen changes over time revealed the fens to be much more dynamic than we anticipated with both aggradation and degradation occurring concurrently in all fens over all time periods, although aggradation was more frequent during the 1978–2003 period. This indicates that permafrost aggradation and degradation is sensitive to both climate and ecological succession, leading to cyclic development of permafrost (Zoltai, 1993). While we are unable to precisely quantify the relative extents of aggradation versus degradation over the last millenium, we interpret that thermokarst fens substantially expanded 300-500 years ago, presumably during Medieval Warming periods, and that permafrost aggraded and transformed much of the fens to birch forests 200-300 years ago, presumably during the Little Ice Age, as indicated by the prevalence of fen peat near the surface of permafrost soils in birch forest (Figure 6) and analyses by Jorgenson et al. (2001). We were not able to detect earlier degradation episodes from the soil stratigraphy, presumably because fen peat from earlier episodes was poorly preserved due to decomposition over time and mixing caused by surface collapse. Recent thermokarst fen expansion (early to midsuccessional stages were common, late stage uncommon) occurred mostly within the last 100 years during the recent era of climate warming. Recent aggradation that we observed since 1949 was common (frequent, but covered little area) before 2003, and rare after 2003. We lack sufficient data to evaluate why permafrost aggraded in some locations and not others.

Most types of permafrost terrain have recently been shown to undergo abrupt thermokarst in response to extreme events, including ice-wedge degradation (Farquharson et al., 2019; Jorgenson, Kanevksiy, et al., 2015; Kanevskiy et al., 2017), active-layer detachment slides (Balser et al., 2014; Lamoureux & Lafrenière, 2009), thermal erosion gullies (Fortier et al., 2007; Toniolo et al., 2009), and thaw slumps (Kokelj et al., 2015; Lewkowicz & Way, 2019). Often the abrupt thermokarst is triggered by high-precipitation events. In contrast, the thermokarst fens have been expanding over centuries.

The range in mean lateral rates of fen expansion we observed of 0.28-0.48 m/yr among the three fens during 1949-2018 was slightly lower that the range in lateral rates of fen expansion of 0.5-1.0 m/yr

JORGENSON ET AL. 16 of 23



roughly estimated by (Jorgenson, 2013). The rates we observed were equivalent to the rates of 0.35–0.39 m/yr for thermokarst lake expansion on the Seward Peninsula over two ~30-yr periods documented by Jones et al. (2011), but somewhat larger that the range of 0.1–0.5 m/yr reported for bogs by Jorgenson (2013). The high variability in mean rates (0.13–0.64 m/yr across fens and periods was surprising, which we attribute to complex fen processes (see ecological discussion below). While seasonal differences in water levels can affect interpretations of fen margins, we think the effect was negligible in our analyses because images were all from midsummer when water levels varied little and the bank heights of fen margins and islands were high (0.5 to 1 m) relative to typical midsummer water-level fluctuations (<0.2 m).

Our remote sensing results, as well as a few field observations, show permafrost aggradation (initially winter season frost that does not thaw the subsequent year) can occur rapidly after a triggering event that freezes the ground 20 to 30 cm below typical active-layer depths. We conclude that it takes only 1 or 2 years of unusually cold winters with little snow to allow frost to penetrate deeply and heave the surface above water. This process then is quickly reinforced by ecological feedbacks that promote further cooling. Our field photos indicate that after heaving of the ground above the water table the hydrophytic sedges and mosses quickly dies (Figure 5). The dead litter then becomes highly reflective to incoming short-wave radiation during summer, and the thick peat helps insulate the permafrost from summer heat input, contributing to further permafrost formation and surface jacking. We cannot envision an alternative scenario where changes in litter, vegetation, or surface water during summer can reduce heat input sufficiently to cause deep frost penetration and surface heaving the subsequent winter. While we have identified numerous individual occurrences of permafrost aggradation within relative narrow time periods, we have not been able to definitively relate the individual occurrences to specific winters because of the insufficient frequency of historical imagery and the sparsity of field monitoring sites that are needed to document the unusual events.

5.2. Climate, Ecological Succession, and Hydrologic Interactions

While a cold climate is the fundamental factor in the formation and preservation of permafrost, the relatively warm permafrost in the boreal zone is strongly influenced by ecological succession, leading to its characterization as ecosystem-driven permafrost (Shur & Jorgenson, 2007). Thus, boreal permafrost formation typically is limited to late successional ecosystems that have tree or shrub canopies that shade the ground and intercept snow, abundant moss cover that insulates the surface, and thick organic soils that affect heat transfer, while lacking surface water that lowers albedo and reduces conductive heat transfer (Jorgenson et al., 2010; Loranty et al., 2018; Viereck, 1970; Zoltai, 1993). Because boreal permafrost is relatively warm $(0^{\circ}\text{C to }-2^{\circ}\text{C})$, it is very sensitive to extreme seasonal temperature and precipitation conditions that substantially alter the soil heat balance. When examining the long-term record for Fairbanks, mean summer air temperatures varied by 4°C across years and mean winter air temperatures varied by 12°C, indicating that winter is by far the stronger driver of long-term soil heat balance. This seasonal difference is as large as the gradient in MAAT across the permafrost affected zones from southwestern Alaska to the Arctic coast. When combined with the effects of average snow depths on the ground during the coldest winter months (NDJFM) that ranged from 11 to 80 cm across years, there were huge differences in thermal effects on soil heat loss between cold, less snowy winters and warm, snowy winters. Thermal modeling by Jorgenson et al. (2010) indicates a difference in 30 cm in snow depths (20 vs. 50 cm) can alter ground temperatures at 2-m depth by 5°C.

We attribute the intermediate-level frequency of permafrost aggradation along the transects in the fens during 1949–1978 (13% of transects) determined by the time series image analysis to the cold, less snowy winters of 1953, 1954, and 1960, the increased frequency during 1978–2003 (27%) to the winters of 1996 and 1999, and the elevated frequency (26%) during 2003–2018 to the winter of 2007. Field observation also revealed heaved mounds with recently dead fen vegetation (colonizing vegetation still absent) on the Tanana Flats in 2001 and 2004 (presumably initiated around 1996–1999. Similarly, in Denali National Park we observed heaved mounds that we believe were initiated by the severe winter of 2007; completely dead vegetation on the mounds was evident on 2010 air photos and coring in 2014 revealed permafrost 1.3 m thick under two of the ~0.5-m-high mounds, but the mounds were not in evident from transect permafrost probing in 2005 or on 2008 satellite imagery. While we were unable to conclusively document that permafrost aggradation and surface heaving on the Tanana Flats responded to those specific years, the limited time series of imagery and field observations strongly support the conclusion that abrupt permafrost aggradation is

JORGENSON ET AL. 17 of 23



caused by extreme winters. Simulations of permafrost dynamics on the Tanana Flats indicated that permafrost reformed after moderate-level fire disturbance during 2000–2010 following late 1990s cooling. While permafrost has aggraded recently and over the past millennium, we believe the more frequent occurrence of warm, wet summers and warm, snowy winters since 2014, as well increased future temperatures and precipitation projected by global climate models (Walsh et al., 2018), indicate that the region has crossed a tipping point where permafrost will no longer form and permafrost loss is irreversible.

Ecological succession after initial permafrost degradation has strong effects of soil thermo-physical properties and heat balance (Jorgenson, Kanevksiy, et al., 2015; Jorgenson et al., 2010; O'Donnell et al., 2012). In fens, we found that over time peat got thicker and denser, which allowed the floating mat to press against the submerged forest soils and elevate the ground surface above the water table. This facilitated a shift from the initial floating aquatic sedges and forbs in relatively deep water to midsuccessional forb species, and eventually to late-successional shrub and moss species without standing water. During this transition, the substantial decrease in water EC indicates groundwater movement primarily effects the collapsing margin with deeper, and often open water, while groundwater flow is reduced through thicker, denser peat founded to the bottom in the late-successional stage formed in the centers of the fens. It is at this stage that the system becomes sensitive to extreme, short-term climate fluctuations. While these general trends were evident from the data, we caution that fens are highly patchy systems with forested islands, fragmented margins, adjacent terrain with variable ice contents, shifting channel patterns, and a historical legacy of past changes that contribute to high variability within the systems. Fire, which is a strong factor in permafrost degradation in adjacent burned forest and scrub ecosystems (Brown et al., 2015) appears to have little effect on fen systems because they do not burn.

Groundwater and surface water are well known to have large effects on the stability of permafrost because of their thermal and physical effects (Hayashi et al., 2011; Jorgenson et al., 2010; Quinton et al., 2009; Walvoord & Kurylyk, 2016). Surface water can raise ground (sediment) temperatures by as much as 12°C and has been shown to be the dominant factor in ice wedge degradation, even in regions with mean annual air temperatures (MAAT) as low as -11°C to -17°C (Farquharson et al., 2019; Jorgenson, Kanevksiy, et al., 2015). Moving water, at or below the surface, can accelerate the degradation as evident in thermal erosion gullies and underground piping even in extremely cold regions (Fortier et al., 2007; Seppälä, 1997; Toniolo et al., 2009). On Tanana Flats the mean annual ground (water) temperature was 3.4°C across all sites during 2012-2014 due to the effects of groundwater, while the MAAT during that period was -2.5°C. Groundwater temperatures of 2-6°C during October through December presumably extended lateral permafrost degradation late into the fall. The heat is particularly important along the degrading permafrost margins of the fens and has resulted in a consistent trend in the long-term lateral degradation rate of 0.36 m/yr with relatively small variation (0.28-0.48 m/yr) among periods. Additionally, partial degradation that can extend tens of meters into the forests beyond the main collapsing margin, as indicated by abundant thermokarst pits, suggests groundwater is affecting deeper thermal regimes. Thus, surface and groundwater strongly predominate over climate as the main driver of permafrost degradation, particularly along the collapsing margins.

The hydrodynamics of fens, and permafrost hydrology more generally, are complicated by the relative roles of snowmelt, seasonal freezing and thawing of the highly conductive organic mat, summer precipitation, groundwater flows, highly patchy forest margins with varying permafrost conditions and hydrologic connections, and highly variable channel widths (Hayashi et al., 2011; Quinton et al., 2009; Walvoord & Kurylyk, 2016). Snowmelt typically is the most dramatic, but short, seasonal phase of the hydrologic cycle causing water levels to abruptly increase (Woo, 2012). At the fens we studied that some of the water ran off quickly due to the frozen surface, but most of the water penetrated through cracks or openings in the ice to provide the initial input that caused the abrupt large increase in water levels that sustained the fens through the summer. Water levels decreased only slightly during early summer when precipitation was typically low and showed only minor increases and short-term responses to high precipitation events during later summer. The increased water levels during early winter when the surface was frozen (no precipitation input) and the gradual, consistent drawdown throughout late winter indicate groundwater input mainly occurred during fall and early winter. Based on the hydroregime and surficial geology evident from Landsat imagery, we conclude the groundwater originates from the Wood River where its channel crosses the coarse glacial outwash fan, consistent with previous interpretations of groundwater discharge fens on the Tanana Flats (Ferrick et al., 2008; Racine & Walters, 1994). Once input into the fen

JORGENSON ET AL. 18 of 23



system, the highly irregular margins and variable channel widths (35–1,147 m in 2003) presumably have large effects on water levels.

5.3. Implications for Ecological Trajectories and Soil Carbon

The highly dynamic patterns of permafrost aggradation and degradation, and the interaction among climate, ecological succession, and hydrology, greatly complicate the projections of ecosystem distribution and soil carbon balance of boreal ecosystems (Douglas et al., 2014; Jorgenson, Marcot, et al., 2015; Pastick et al., 2018; Quinton et al., 2011). Projections of future ecological transitions in boreal lowlands are challenging given the highly dynamic processes associated with both permafrost and hydrology of the fens. Pastick et al. (2015) projected nearly all the permafrost on the Tanana Flats would be lost by 2090 based on GIS statistical modeling. Based on past historical rates of birch and spruce forest loss associated with permafrost degradation, birch forests that frequently are associated with ice-rich permafrost will likely be lost by 2100 (Jorgenson et al., 2001; Lara et al., 2015). While nearly complete permafrost degradation is highly likely, what the landscape will become in the future is uncertain. Patterns of ecological succession and peat accumulation likely will allow birch and black spruce woodlands, as well as dwarf birch-willow scrublands, to predominate across the new permafrost free landscape. Alternatively, as permafrost degrades, fens expand, and summers become warmer and wetter, the entire landscape could come to resemble the landscape of the Susitna Valley in the southern boreal zone with its extensive fen peatlands (Aapa-mires) with stable upraised islands (Loisel & Yu, 2013). Thus, in this extremely low gradient terrain, the interplay between expanding channel widths and configurations, channelization that alters surface versus subsurface flow, precipitation and temperature changes, and peat accumulation rates could greatly affect future ecological transitions.

Permafrost degradation in peat-rich soils has been projected to substantially increase emissions of carbon dioxide and methane to the atmosphere, creating a positive feedback where climate warming accelerates permafrost thaw (McGuire et al., 2018; Schuur et al., 2015). These projections generally rely on estimates of the soil carbon pool (Hugelius et al., 2014), the areal extent of thawing permafrost (Chadburn et al., 2017), the portion of the soil carbon pool likely to thaw and be susceptible to increased decomposition (Harden et al., 2012; Olefeldt et al., 2016; Ping et al., 2015), and microcosm experiments that quantify carbon emissions from thawed soils (Ping et al., 2015). Our results indicate that permafrost dynamics in highly heterogeneous boreal peatlands greatly complicate the currently simplistic projections of soil carbon loss after thawing. We identify four factors that provide caution in accepting the assumptions underlying currently available projections. First, much of the permafrost in the boreal zone has already degraded (Jorgenson et al., 2001; Jorgenson, Shur, et al., 2007; Kanevskiy et al., 2014; Thie, 1974). Within the boreal region of central Alaska, Jorgenson, Shur, et al. (2007) found that permafrost occurred on 67% of the total area and 7% of permafrost-affected areas had thermokarst. Thus, substantial carbon emissions from thawing soils have already been occurring over the past centuries and contributed to "baseline" atmospheric conditions. Second, boreal ecosystems are a highly patchy mosaic undergoing permafrost degradation and postthermokarst succession, leading to patches of early successional ecosystems generally losing soil carbon, while late-successional ecosystems gain carbon in new peat (Jones et al., 2017; Jorgenson et al., 2013; Klein et al., 2013). We found soil carbon accumulated at a rate of 0.06 kg/m²/yr over about 250 years, although we did not compare carbon contents of new peat versus old peat to adequately quantify overall soil carbon change over time. Third, our results and others (Kanevskiy et al., 2014; Zoltai, 1993) show much of current permafrost in boreal lowlands has undergone at least one, and sometime multiple episodes of permafrost aggradation and degradation. Thus, the deep carbon has already undergone long periods of degradation that would reduce the lability of the soil carbon. In our permafrost cores, the organic soils in permafrost usually were moderately decomposed (mucky peat), indicating they had already undergone substantial decomposition. Fourth, after collapse and subsequent decades to centuries of ecological succession the old peat becomes waterlogged and much denser under substantial pressure from surface water, thus, creating a very poor environment for gas, water, and nutrient exchange required for decomposition. Thus, boreal peatlands provide a good environment for long-term accumulation of peat across a broad climatic gradient (Loisel & Yu, 2013; Yu et al., 2010). These are all significant factors, but they are not adequately accounted for in current biome-wide projections of the soil carbon balance.

JORGENSON ET AL. 19 of 23



6. Conclusions

Groundwater is the primary driver of permafrost degradation in lowland fen systems on Tanana Flats of central Alaska due to the relatively warm near-surface water that continues to deliver heat to adjacent permafrost soils through early winter. We found that new permafrost was formed during the last several decades in a small portion of the fens, primarily due to large annual climate variations that include extreme summer and winter conditions favorable for permafrost formation. However, permafrost aggradation only occurred in late-successional ecosystems. Repeated permafrost aggradation and degradation also was evident in permafrost cores. The successional shift in plant species and growth forms, peat accumulation, and decreasing relative water levels produce thermophysical conditions favorable to permafrost aggradation during periods of extremely cold, less snowier winters. Thus, the highly dynamic patterns of repeated permafrost aggradation and degradation, and the interaction among climate, ecological succession, and hydrology greatly complicate projections of ecosystem distribution and soil carbon balance of boreal ecosystems. The overall trend of gradual thermokarst fen expansion, more frequent warm, snowy winters since 2014, and model projections for warmer winters, however, indicate that the region has crossed a tipping point where permafrost will no longer form and permafrost loss is irreversible.

Conflict of Interest

There are no conflicts of interest for any author.

Data Availability Statement

The data are publicly available at https://portal.edirepository.org/nis/mapbrowse?scope=edi&identifier=628&revision=1.

Acknowledgments References

funded by the Department of Defense's Strategic Environmental Research and Development Program (Projects RC-2110 and 18-1170) and the U.S. Army Corps of Engineers Engineer Research and Development Center's Basic Research (6.1) Program. Earlier projects related to the Ft. Wainwright ecological land survey and airboat disturbance studies were funded by the U.S. Army Alaska. D. Rees helped with helicopter logistics and field measurements. We thank Amanda Barker, Dana Brown, Art Gelvin, and Karen Jorgenson for help with field measurements. Chuck Racine has been

included posthumously. The comments

of two anonymous reviewers were

appreciated.

The recent portion of this research was

Balser, A. W. (1996). Combining Landsat TM and multi-temporal ERS-1 imagery to improve classification accuracy and detail in the Tanana Flats wetlands complex, interior Alaska (M.S. Thesis). Fairbanks, AK: University of Alaska. https://jlc-web.uaa.alaska.edu

- Balser, A. W., Jones, J. B., & Gens, R. (2014). Timing of retrogressive thaw slump initiation in the Noatak Basin, Northwest Alaska, USA. Journal of Geophysical Research: Earth Surface, 119, 1106–1120. https://doi.org/10.1002/2013JF002889
- Barker, A. J., Douglas, T. A., Jacobson, A. D., McClelland, J. W., Ilgen, A. G., Khosh, M. S., et al. (2014). Late season mobilization of trace metals in two small Alaskan arctic watersheds as a proxy for landscape scale permafrost active layer dynamics. *Chemical Geology*, 381, 180–193. https://doi.org/10.1016/j.chemgeo.2014.05.012
- Boertje, R. D., Seaton, C. T., Young, D. D., Keech, M. A., & Dale, B. W. (2000). Factors limiting moose at high densities in Unit 20A (Federal aid in wildlife restoration research performance report, July 1999–June 2000. Grant W-27-3, study 1.51). Juneau, AK: Alaska Department of Fish and Game. http://www.adfg.alaska.gov/static/research/programs/intensivemanagement/pdfs/refs/1.51_00.pdf
- Brown, D. R. N., Jorgenson, M. T., Douglas, D. C., Romanovsky, V., Kielland, K., Hiemstra, C., et al. (2015). Interactive effects of wildfire and climate on permafrost degradation in Alaskan lowland forests. *Journal of Geophysical Research: Biogeosciences*, 120, 1619–1637. https://doi.org/10.1002/2015JG003033
- Bubier, J. L. (1995). The relationship of vegetation to methane emission and hydrochemical gradients in northern peatlands. *Journal of Ecology*, 83, 403–420. https://www.jstor.org/stable/2261594
- Burn, C. R., & Jorgenson, M. T. (2020). Permafrost in the northwest boreal region. In C. Markon, et al. (Eds.), *Drivers of landscape change in the northwest boreal region* (pp. 51–57). Fairbanks, AK: University of Alaska Press. https://press.uchicago.edu/ucp/books/book/distributed/D/bo45711596.html
- Chadburn, S. E., Burke, E. J., Cox, P. M., Friedlingstein, P., Hugelius, G., & Westermann, S. (2017). An observation-based constraint on permafrost loss as a function of global warming. *Nature Climate Change*, 7(5), 340–344. https://doi.org/10.1038/nclimate3262
- Douglas, T. A., Blum, J. D., Guo, L., Keller, K., & Gleason, J. D. (2013). Hydrogeochemistry of seasonal flow regimes in the Chena River, a subarctic watershed draining discontinuous permafrost in interior Alaska (USA). *Chemical Geology*, 335, 48–62. https://doi.org/10.1016/j.chemgeo.2012.10.045
- Douglas, T. A., Jones, M. C., Hiemstra, C. A., & Arnold, J. (2014). Sources and sinks of carbon in boreal ecosystems of interior Alaska: Current and future perspectives for land managers. *Elementa: Science of the Anthropocene*, 2(39). http://doi.org/10.12952/journal. elementa.000032
- Douglas, T. A., Jorgenson, M. T., Brown, D. R. N., Campbell, S., Hiemstra, C., Saari, S., et al. (2015). Degrading permafrost mapped with electrical resistivity tomography, airborne imagery and LiDAR, and seasonal thaw measurements. *Geophysics*, 81(1), WA71–WA85. https://doi.org/10.1190/geo2015-0149.1
- Douglas, T. A., Turetsky, M. R., & Koven, C. D. (2020). Increased rainfall stimulates permafrost thaw across a variety of interior Alaskan boreal ecosystems. *Nature Climate and Atmospheric Change*, 3(1), 1–7. https://doi.org/10.1038/s41612-020-0130-4
- Fan, Y., Li, H., & Miguez-Macho, G. (2013). Global patterns of groundwater table depth. Science, 339(6122), 940–943. https://doi.org/
- Farquharson, L. M., Romanovsky, V. E., Cable, W. L., Walker, D. A., Kokelj, S., & Nicolsky, D. (2019). Climate change drives widespread and rapid thermokarst development in very cold permafrost in the Canadian High Arctic. *Geophysical Research Letters*, 46, 6681–6689. https://doi.org/10.1029/2019GL082187

JORGENSON ET AL. 20 of 23



- Ferrick, M. G., Racine, C. H., Reidsma, S., Saari, S. P., Gelvin, A. B., Collins, C. M., & Larsen, G. (2008). Temperatures and water levels at Tanana Flats Monitoring Stations (ERDC/CRREL TR-08-8). Hanover, NH: Cold Regions Research and Engineering Laboratory. https://erdc-library.erdc.dren.mil/jspui/bitstream/11681/5314/1/CRREL-TR-08-8.pdf
- Field, C. B., Barros, V., Stocker, T. F., Qin, D., Dokken, D. J., Ebi, K. L., et al. (2012). Managing the risks of extreme events and disasters to advance climate change adaptation (Special Report of Working Groups I and II of the Intergovernmental Panel on Climate Change). Cambridge, UK: Cambridge University Press. Retrieved from https://www.ipcc.ch/site/assets/uploads/2018/03/SREX_Full_Report-1.pdf
- Fortier, D., Allard, M., & Shur, Y. (2007). Observation of rapid drainage system development by thermal erosion of ice wedges on Bylot Island, Canadian Arctic Archipelago. *Permafrost and Periglacial Processes*, 18(3), 229–243. https://doi.org/10.1002/ppp.595
- French, H. M., & Shur, Y. (2010). The principles of cryostratigraphy. *Earth-Science Reviews*, 101, 190. Retrieved From https://doi.org/10.1016/j.earscirev.2010.04.002
- Glagolev, M., Kleptsova, I., Filippov, I., Maksyutov, S., & Machida, T. (2011). Regional methane emission from West Siberia mire land-scapes. *Environmental Research Letters*, 6(4), 045214. https://iopscience.iop.org/article/10.1088/1748-9326/6/4/045214/meta
- Harden, J. W., Koven, C. D., Ping, C.-L., Hugelius, G., McGuire, A. D., Camill, P., et al. (2012). Field information links permafrost carbon to physical vulnerabilities of thawing. *Geophysical Research Letters*, 39, L15704. https://doi.org/10.1029/2012GL051958
- Hayashi, M., McClymont, A. F., Christensen, B. S., Bentley, L. R., & Quinton, W. L. (2011). Thawing of permafrost peatlands: Effects of water-energy feedback on landscape evolution. In Proceedings of the Joint Meeting of the International Association of Hydrogeologists Canadian National Chapter and the Canadian Quaternary Association (pp. 1–5). Richmond, BC: IAH-CNC. Retrieved from https://pdfs. semanticscholar.org/dff9/34376fc8413d1be1f7a5119346a0143c8784.pdf
- Hayashi, M., Quinton, W. L., Pietroniro, A., & Gibson, J. J. (2004). Hydrologic functions of wetlands in a discontinuous permafrost basin indicated by isotopic and chemical signatures. *Journal of Hydrology*, 296, 81–97. https://doi.org/10.1016/j.jhydrol.2004.03.020
- Hugelius, G., Strauss, J., Zubrzycki, S., Harden, J. W., Schuur, E. A. G., Ping, C. L., et al. (2014). Estimated stocks of circumpolar permafrost carbon with quantified uncertainty ranges and identified data gaps. *Biogeosciences*, 11(23), 6573–6593. https://doi.org/10.5194/bg-11-6573-2014
- Jepsen, S. M., Voss, C. I., Walvoord, M. A., Minsley, B. J., & Rover, J. (2013). Linkages between lake shrinkage/expansion and sublacustrine permafrost distribution determined from remote sensing of interior Alaska, USA. Geophysical Research Letters, 40, 1–6. https://doi.org/ 10.1002/grl.50187
- Jones, B. M., Grosse, G., Arp, C. D., Jones, M. C., Walter Anthony, K. M., & Romanovsky, V. E. (2011). Modern thermokarst lake dynamics in the continuous permafrost zone, northern Seward Peninsula, Alaska. *Journal of Geophysical Research*, 116, G00M03. https://doi.org/ 10.1029/2011JG001666
- Jones, M. C., Harden, J., O'Donnell, J., Manies, K., Jorgenson, T., Treat, C., & Ewing, S. (2017). Rapid carbon loss and slow recovery following permafrost thaw in boreal peatlands. *Global Change Biology*, 23(3), 1109–1127. https://doi.org/10.1111/gcb.13403
- Jorgenson, M. T. (2013). Thermokarst terrains. In J. Schroeder, R. Giardino, J. Harbor (Eds.), *Treatise on Geomorphology 8 Glacial and Periglacial Geomorphology* (pp. 313–324). San Diego: Academic Press. https://www.academia.edu/25248005/
- Jorgenson, M. T., Harden, J., Kanevskiy, M., O'Donnel, J., Wickland, K., Ewing, S., et al. (2013). Reorganization of vegetation, hydrology and soil carbon after permafrost degradation across heterogeneous boreal landscapes. *Environmental Research Letters*, 8(3), 035017. https://doi.org/10.1088/1748-9326/8/3/035017
- Jorgenson, M. T., Kanevskiy, M., Shur, Y., Moskalenko, N., Brown, D. R. N., Wickland, K., et al. (2015). Role of ground-ice dynamics and ecological feedbacks in recent ice-wedge degradation and stabilization. *Journal of Geophysical Research: Earth Surface*, 120, 2280–2297. https://doi.org/10.1002/2015JF003602
- Jorgenson, M. T., Marcot, B. G., Swanson, D. K., Jorgenson, J. C., & DeGange, A. R. (2015). Projected changes in diverse ecosystems from climate warming and biophysical drivers in Northwest Alaska. *Climatic Change*, 130(2), 131–144. https://doi.org/10.1007/s10584-014-1202.1
- Jorgenson, M. T., Murphy, S. M., Roth, J. E., Cater, T. C., Obritschkewitsch, T. A., Frost, G. V., et al. (2007). Investigations of impacts to fen ecosystems and wildlife from airboat traffic on the Tanana flats, Fort Wainwright, Alaska, 2002–2006. (Unpublished report prepared for U.S. Army Alaska, Fort Richardson, Anchorage, AK, by ABR, Inc. and Far North Aquatics, Fairbanks, AK).
- Jorgenson, M. T., Racine, C. H., Walters, J. C., & Osterkamp, T. E. (2001). Permafrost degradation and ecological changes associated with a warming climate in Central Alaska. Climatic Change, 48(4), 551–579. https://doi.org/10.1023/A:1005667424
- Jorgenson, M. T., Romanovsky, V., Harden, J., Shur, Y., O'Donnell, J., Schuur, E. A. G., et al. (2010). Resilience and vulnerability of permafrost to climate change. Canadian Journal of Forest Research, 40(7), 1219–1236. https://doi.org/10.1139/X10-060
- Jorgenson, M. T., Roth, J. E., Raynolds, M., Smith, M. D., Lentz, W., Zusi-Cobb, A., & Racine, C. H. (1999). An ecological land survey for Fort Wainwright, Alaska (CRREL Report 99–9). Hanover, NH: U.S. Army Cold Regions Research and Engineering Laboratory. https://erdc-library.erdc.dren.mil/jspui/bitstream/11681/9249/1/CR-99-9.pdf
- Jorgenson, M. T., Shur, Y. L., Osterkamp, T. E., & George, T. (2007). Nature and extent of permafrost degradation in the discontinuous permafrost zone of Alaska. In *Proceedings of Seventh International Conference on Global Change: Connection to the Arctic (GCCA-7)* (pp. 120–125). Fairbanks, AK: International Arctic Research Center, University of Alaska. https://jlc-web.uaa.alaska.edu
- Kane, E. S., Turetsky, M. R., Harden, J. W., McGuire, A. D., & Waddington, J. M. (2010). Seasonal ice and hydrologic controls on dissolved organic carbon and nitrogen concentrations in a boreal rich fen. *Journal of Geophysical Research*, 115, G04012. https://doi.org/10.1029/ 2010JG001366
- Kanevskiy, M., Jorgenson, T., Shur, Y., O'Donnell, J. A., Harden, J. W., Zhuang, Q., & Fortier, D. (2014). Cryostratigraphy and permafrost evolution in the lacustrine lowlands of west-Central Alaska. *Permafrost and Periglacial Processes*, 25(1), 14–34. https://doi.org/10.1002/ ppp.1800
- Kanevskiy, M., Shur, Y., Jorgenson, T., Brown, D. R., Moskalenko, N., Brown, J., et al. (2017). Degradation and stabilization of ice wedges: Implications for assessing risk of thermokarst in northern Alaska. *Geomorphology*, 297, 20–42. https://doi.org/10.1016/j.geomorph.2017.09.001
- Klein, E. S., Yu, Z., & Booth, R. K. (2013). Recent increase in peatland carbon accumulation in a thermokarst lake basin in southwestern Alaska. *Palaeogeography, Palaeoclimatology, Palaeoecology, 392*, 186–195. https://doi.org/10.1016/j.palaeo.2013.09.009
- Kokelj, S. V., Tunnicliffe, J., Lacelle, D., Lantz, T. C., Chin, K. S., & Fraser, R. (2015). Increased precipitation drives mega slump development and destabilization of ice-rich permafrost terrain, northwestern Canada. Global and Planetary Change, 129, 56–68. https://doi.org/10.1016/i.gloplacha.2015.02.008
- Lamoureux, S. F., & Lafrenière, M. J. (2009). Fluvial impact of extensive active layer detachments, Cape Bounty, Melville Island, Canada. Arctic, Antarctic, and Alpine Research, 41(1), 59–68. https://doi.org/10.1657/1523-0430-41.1.59

JORGENSON ET AL. 21 of 23



- Lara, M. J., Genet, H., McGuire, A. D., Euskirchen, E. S., Zhang, Y., Brown, D., et al. (2015). Thermokarst rates intensify due to climate change and forest fragmentation in an Alaskan boreal forest lowland. *Global Change Biology*, 22(2), 816–829. https://doi.org/10.1111/gcb.13124
- Lewkowicz, A. G., & Way, R. G. (2019). Extremes of summer climate trigger thousands of thermokarst landslides in a high Arctic environment. *Nature Communications*, 10(1), 1329. https://doi.org/10.1038/s41467-019-09314-7
- Liljedahl, A. K., Boike, J., Daanen, R. P., Fedorov, A. N., Frost, G. V., Grosse, G., et al. (2016). Pan-Arctic ice-wedge degradation in warming permafrost and its influence on tundra hydrology. *Nature Geoscience*, 9(4), 312–318. https://doi.org/10.1038/ngeo2674
- Lindholm, T., & Heikkilä, R. (2006). Finland—Land of mires (Vol. The Finnish environment 23): Finnish Environment Institute. http://hdl.handle.net/10138/37961
- Liston, G. E., & Hiemstra, C. A. (2011). The changing cryosphere: Pan-Arctic snow trends (1979–2009). *Journal of Climate*, 24(21), 5691–5712. https://doi.org/10.1175/JCLI-D-11-00081.1
- Loisel, J., & Yu, Z. (2013). Recent acceleration of carbon accumulation in a boreal peatland, south Central Alaska. *Journal of Geophysical Research: Biogeosciences*, 118, 41–53. https://doi.org/10.1029/2012JG001978
- Loranty, M. M., Abbott, B. W., Blok, D., Douglas, T. A., Epstein, H. E., Forbes, B. C., et al. (2018). Reviews and syntheses: Changing ecosystem influences on soil thermal regimes in northern high-latitude permafrost regions. *Biogeosciences*, 15(17), 5287–5313. https://doi.org/10.5194/bg-15-5287-2018
- McGuire, A. D., Lawrence, D. M., Koven, C., Clein, J. S., Burke, E., Chen, G., et al. (2018). Dependence of the evolution of carbon dynamics in the northern permafrost region on the trajectory of climate change. *PNAS*, 115(15), 3882–3887. https://doi.org/10.1073/pnas.1719903115
- NWWG (1988). Wetlands of Canada, Ecological Land Classification Series, No. 24. Montreal, Quebec: National Wetlands Working Group, Environment Canada.
- O'Donnell, J. A., Jorgenson, M. T., Harden, J. W., McGuire, A. D., Kanevskiy, M. Z., & Wickland, K. P. (2012). The effects of permafrost thaw on soil hydrologic, thermal and carbon dynamics in an Alaskan peatland. *Ecosystems*, 15, 213–229. https://doi.org/10.1007/s10021-011-9504-0
- Olefeldt, D., Goswami, S., Grosse, G., Hayes, D. J., Hugelius, G., Kuhry, P., et al. (2016). Circumpolar distribution and carbon storage of thermokarst landscapes. *Nature Communications*, 7(1), 1–11. https://doi.org/10.3334/ORNLDAAC/1332
- Olefeldt, D., & Roulet, N. T. (2014). Permafrost conditions in peatlands regulate magnitude, timing, and chemical composition of catchment dissolved organic carbon export. *Global Change Biology*, 20(10), 3122–3136. https://doi.org/10.1111/gcb.12607
- Osterkamp, T. E., Viereck, L., Shur, Y., Jorgenson, M. T., Racine, C., Doyle, A., & Boone, R. D. (2000). Observations of thermokarst and its impact on boreal forests in Alaska, U.S.A. Arctic, Antarctic, and Alpine Research, 32(3), 303–315. https://doi.org/10.1080/15230430.2000.12003368
- Pastick, N. J., Jorgenson, M. T., Goetz, S. J., Jones, B. M., Wylie, B. K., Minsley, B. J., et al. (2018). Spatiotemporal remote sensing of ecosystem change and causation across Alaska. Global Change Biology, 25(3), 1171–1189. https://doi.org/10.1111/gcb.14279
- Pastick, N. J., Jorgenson, M. T., Wylie, B. K., Nield, S. J., Johnson, K. D., & Finley, A. O. (2015). Distribution of near-surface permafrost in Alaska: Estimates of present and future conditions. *Remote Sensing of Environment*, 168, 301–315. https://doi.org/10.1016/j. rse.2015.07.019
- Payette, S., Delwaide, A., Caccianiga, M., & Beauchemin, M. (2004). Accelerated thawing of subarctic peatland permafrost over the last 50 years. *Geophysical Research Letters*, 31, L18208. https://doi.org/10.1029/2004GL020358
- Petrone, K. C., Jones, J. B., Hinzman, L. D., & Boone, R. D. (2006). Seasonal export of carbon, nitrogen, and major solutes from Alaskan catchments with discontinuous permafrost. *Journal of Geophysical Research*, 111, G02020. https://doi.org/10.1029/2005JG000055
- Ping, C. L., Jastrow, J. D., Jorgenson, M. T., Michaelson, G. J., & Shur, Y. L. (2015). Permafrost soils and carbon cycling. The Soil, 1(1), 147–171. https://doi.org/10.5194/soild-1-709-2014
- Quinton, W. L., Hayashi, M., & Carey, S. K. (2008). Peat hydraulic conductivity in cold regions and its relation to pore size and geometry. Hydrological Processes: An International Journal, 22(15), 2829–2837. https://doi.org/10.1002/hyp.7027
- Quinton, W. L., Hayashi, M., & Chasmer, L. (2009). Peatland hydrology of discontinuous permafrost in the Northwest Territories: Overview and synthesis. Canadian Water Resources Journal, 34, 311–328. https://doi.org/10.4296/cwrj3404311
- Quinton, W. L., Hayashi, M., & Chasmer, L. E. (2011). Permafrost-thaw-induced land-cover change in the Canadian subarctic: Implications for water resources. *Hydrological Processes*, 25, 152–158. https://doi.org/10.1002/hyp.7894
- Quinton, W. L., Hayashi, M., & Pietroniro, A. (2003). Connectivity and storage functions of channel fens and flat bogs in northern basins. Hydrological Processes, 17(18), 3665–3684. https://doi.org/10.1002/hyp.1369
- Racine, C. H., Jorgenson, M. T., & Walters, J. C. (1998). Thermokarst vegetation in lowland birch forests on the Tanana Flats, interior Alaska, U.S.A. In A. G. Lewkowicz & M. Allard (Eds.), Proceedings of Seventh International Conference on Permafrost (Collection Nordicana (Vol. 57, pp. 927–933). Sainte-Foy, Quebec: Universite Laval. http://www.cen.ulaval.ca/nordicanad/donnees/nordicana/ Nordicana57_464036ND.pdf
- Racine, C. H., & Walters, J. C. (1994). Groundwater-discharge fens in the Tanana lowlands, interior Alaska, U.S.A. Arctic and Alpine Research, 26(4), 418–426. https://www.tandfonline.com/doi/abs/10.1080/00040851.1994.12003087
- Racine, C. H., Walters, J. C., & Jorgenson, M. T. (1998). Airboat use and disturbance of floating mat fen wetlands in interior Alaska, U.S.A. Arctic, 51(4), 371–377. https://www.jstor.org/stable/40511855
- Roach, J., Griffith, B., Verbyla, D., & Jones, J. (2011). Mechanisms influencing changes in lake area in the Alaskan boreal forest. *Global Change Biology*, 17(8), 2567–2583. https://doi.org/10.1111/j.1365-2486.2011.02446.x
- Rober, A. R., Wyatt, K. H., Stevenson, R. J., & Turetsky, M. R. (2014). Spatial and temporal variability of algal community dynamics and productivity in floodplain wetlands along the Tanana River, Alaska. Freshwater Science, 33(3), 765–777. https://doi.org/10.1086/ 676939
- Roulet, N., Moore, T. I. M., Bubier, J., & Lafleur, P. (1992). Northern fens: Methane flux and climatic change. *Tellus B*, 44(2), 100–105. https://doi.org/10.1034/j.1600-0889.1992.t01-1-00002.x
- Runyan, C. W., & D'Odorico, P. (2012). Ecohydrological feedbacks between permafrost and vegetation dynamics. Advances in Water Resources, 49, 1–12. https://doi.org/10.1016/j.advwatres.2012.07.016
- Schuur, E. A. G., McGuire, A. D., Schädel, C., Grosse, G., Harden, J. W., Hayes, D. J., et al. (2015). Climate change and the permafrost carbon feedback. *Nature*, 520(7546), 171–179. https://doi.org/10.1038/nature14338
- Seppälä, M. (1997). Piping causing thermokarst in permafrost, Ungava peninsula, Quebec, Canada. *Geomorphology*, 20(3–4), 313–319. https://doi.org/10.1016/S0169-555X(97)00032-9

JORGENSON ET AL. 22 of 23



- Shur, Y. L., & Jorgenson, M. T. (2007). Patterns of permafrost formation and degradation in relation to climate and ecosystems. *Permafrost and Periglacial Processes*, 18, 7–19. https://doi.org/10.1002/ppp.582
- Sjöberg, Y., Coon, E., Sannel, A. B. K., Pannetier, R., Harp, D., Frampton, A., et al. (2016). Thermal effects of groundwater flow through subarctic fens: A case study based on field observations and numerical modeling. *Water Resources Research*, 52, 1591–1606. https://doi.org/10.1002/2015WR017571
- Sulman, B. N., Desai, A. R., Saliendra, N. Z., Lafleur, P. M., Flanagan, L. B., Sonnentag, O., et al. (2010). CO₂ fluxes at northern fens and bogs have opposite responses to inter-annual fluctuations in water table. *Geophysical Research Letters*, 37, L19702. https://doi.org/10.1029/2010GL044018
- Thie, J. (1974). Distribution and thawing of permafrost in the southern part of the discontinuous zone in Manitoba. *Arctic*, 27, 189–200. https://www.jstor.org/stable/40509225
- Toniolo, H., Kodial, P., Hinzman, L. D., & Yoshikawa, K. (2009). Spatio-temporal evolution of a thermokarst in interior Alaska. Cold Regions Science and Technology, 56, 39–49. https://doi.org/10.1016/j.coldregions.2008.09.007
- Turetsky, M. R., Treat, C. C., Waldrop, M. P., Waddington, J. M., Harden, J. W., & McGuire, A. D. (2008). Short-term response of methane fluxes and methanogen activity to water table and soil warming manipulations in an Alaskan peatland. *Journal of Geophysical Research*, 113, G00A10. https://doi.org/10.1029/2007JG000496
- Viereck, L. A. (1970). Forest succession and soil development adjacent to the Chena River in interior Alaska. *Arctic and Alpine Research*, 2(1), 1–26. https://www.tandfonline.com/doi/abs/10.1080/00040851.1970.12003558
- Vonk, J. E., Tank, S. E., & Walvoord, M. A. (2019). Integrating hydrology and biogeochemistry across frozen landscapes. *Nature Communications*, 10(1), 1–4. https://doi.org/10.1038/s41467-019-13361-5
- Walsh, J. E., Bhatt, U. S., Littell, J. S., Leonawicz, M., Lindgren, M., Kurkowski, T. A., et al. (2018). Downscaling of climate model output for Alaskan stakeholders. Environmental Modelling & Software, 110, 38–51. https://doi.org/10.1016/j.envsoft.2018.03.021
- Walters, J. C., Racine, C. H., & Jorgenson, M. T. (1998). Characteristic of permafrost in the Tanana Flats, interior Alaska. In A. G. Lewkowicz & M. Allard (Eds.), *Proceedings of Seventh International Conference on Permafrost Collection Nordicana* (Vol. 57, pp. 1109–1116). Sainte-Foy, Quebec: Universite Laval. http://www.cen.ulaval.ca/nordicanad/donnees/nordicana/Nordicana57_
- Walvoord, M. A., & Kurylyk, B. L. (2016). Hydrologic impacts of thawing permafrost: A review. *Vadose Zone Journal*, 15(6). https://doi.org/10.2136/vzj2016.01.0010
- Walvoord, M. A., & Striegl, R. G. (2007). Increased groundwater to stream discharge from permafrost thawing in the Yukon River basin: Potential impacts on lateral export of carbon and nitrogen. *Geophysical Research Letters*, 34, L12402. https://doi.org/10.1029/2007GL030216
- Wolken, J. M., Hollingsworth, T. N., Rupp, T. S., Chapin, F. S. III, Trainor, S. F., Barrett, T. M., et al. (2011). Evidence and implications of recent and projected climate change in Alaska's forest ecosystems. *Ecosphere*, 2(11), art124. https://doi.org/10.1890/ES11-00288.1 Woo, M.-K. (2012). *Permafrost Hydrology*. Berlin: Springer-Verlag.
- Wright, N., Hayashi, M., & Quinton, W. L. (2009). Spatial and temporal variations in active layer thawing and their implication on runoff generation in peat-covered permafrost terrain. Water Resources Research, 45, W05414. https://doi.org/10.1029/2008WR006880
- Yoshikawa, K., & Hinzman, L. D. (2003). Shrinking thermokarst ponds and groundwater dynamics in discontinuous permafrost near council, Alaska. *Permafrost and Periglacial Processes*, 14(2), 151–160. https://doi.org/10.1002/ppp.451
- Yu, Z. C., Loisel, J., Brosseau, D. P., Beilman, D. W., & Hunt, S. J. (2010). Global peatland dynamics since the Last Glacial Maximum. Geophysical Research Letters, 37, L13402. https://doi.org/10.1029/2010GL043584
- Zoltai, S. C. (1993). Cyclic development of permafrost in the peatlands of northwestern Alberta, Canada. *Arctic and Alpine Research*, 25, 240–246. https://www.tandfonline.com/doi/abs/10.1080/00040851.1993.12003011

JORGENSON ET AL. 23 of 23